

Universitat de Lleida

Document downloaded from:

<http://hdl.handle.net/10459.1/66708>

The final publication is available at:

<https://doi.org/10.1016/j.enconman.2019.112060>

Copyright

cc-by-nc-nd, (c) Elsevier, 2019



Està subjecte a una llicència de [Reconeixement-NoComercial-SenseObraDerivada 4.0 de Creative Commons](https://creativecommons.org/licenses/by-nc-nd/4.0/)

Gas engine heat pump system: experimental facility and thermal evaluation for 5 different units

Authors: José Sánchez Ramos^a, MCarmen Guerrero Delgado^b, Servando Álvarez Domínguez^b, José Luis Molina Félix^b, Luisa F. Cabeza^c

^a Thermal machines and engines, School of engineer, Av. University of Cádiz, 10, 11519, Puerto Real, Spain

^b Department of energy engineering. School of engineer. University of Seville. Camino de los Descubrimientos s/n, 41092 Seville, Spain.

^c GREiA Research Centre, INSPIRES Research Centre, Universitat de Lleida, Pere de Cabrera s/n, 25001 Lleida

Abstract

Gas Engine Heat Pump requires simplified characterization models that allow evaluating its economic and energy impacts. These simplified solutions can be implemented in complex simulation algorithms for different commercial solutions with a low computational cost.

The study aims to develop a simplified characterization model highly accurate, easy to reproduce and apply. The methodology carried out uses an experimental installation to analyze different units tested under different operating conditions. With the results of the carried out experimentation, it will be possible to know the real thermal response of these HVAC systems and to develop the simplified characterization model based on operating curves. The thermal behaviour of the systems could be evaluated using the defined curves under any operating condition of the GEHP system. Moreover, they are based on parameters available in the manufacturer datasheets.

The results of the validation show that this model is highly accurate. It has a maximum error of 25% and an average error of less than 7%. Also, the formulation shows that it is easy to reproduce and to apply. Last, uncertainty analysis shows reasonable confidence in the identified performance curves.

Keywords: Gas engine-driven heat pump, experimental model, waste heat recovery, thermal characterization, inverse modelling

30 0 Nomenclature

Variable/Acronym/ Abbreviation	Description	Units
GEHP	Gas Engine Heat Pump	-
EPBD	Energy Performance of Buildings Directive	-
NZEB	Nearly Zero Energy Buildings	-
EHP	Electric Heat Pump	-
EER	Energy Efficient Ratio	-
COP	Coefficient Of Performance	-
SEER	Seasonal Energy Efficient Ratio	-
SCOP	Seasonal Coefficient Of Performance	-
m_w	Water flow	kg/s
PLR	Part load ratio	%
$T_{LIM-REC}$	Minimum outdoor temperature to put on recovery system of GEHP	°C
DHW	Domestic Hot Water	-
$T_{SETPOINT}$	Setpoint temperature	°C
$Q_{RECOVERY}$	Recovery heat from cooling system of engine	kW
T_{ow}	Outlet water temperature	°C
T_{iw}	Inlet water temperature	°C
T_{dr}	Outdoor dry-bulb temperature	°C
T_{wb}	Outdoor wet-bulb temperature	°C
$Heat_{real}$	Heat capacity in real operation conditions	kW
$Heat_{nom}$	Heat capacity in nominal operation conditions	kW
$ConGasH_{real}$	Gas consumption in heating mode in real operation conditions	kW
$ConGasH_{nom}$	Gas consumption in heating mode in nominal operation conditions	kW
$ConElecH_{real}$	Electrical consumption in heating mode in real operation conditions	kW
$ConElecH_{nom}$	Electrical consumption in heating mode in nominal operation conditions	kW
$RecQH_{real}$	Heat recoverable in heating mode in real operation conditions	kW
$RecQH_{nom}$	Heat recoverable in heating mode in nominal operation conditions	kW
$Cold_{real}$	Cooling capacity in real operation conditions	kW
$Cold_{nom}$	Cooling capacity in nominal operation conditions	kW
$ConGasC_{real}$	Gas consumption in cooling mode in real operation conditions	kW
$ConGasC_{nom}$	Gas consumption in cooling mode in nominal operation conditions	kW
$ConElecC_{real}$	Electrical consumption in cooling mode in real operation conditions	kW
$ConElecC_{nom}$	Electrical consumption in cooling mode in nominal operation conditions	kW
$RecQC_{real}$	Heat recoverable in cooling mode in real operation conditions	kW
$RecQC_{nom}$	Heat recoverable in cooling mode in nominal operation conditions	kW
T_{orec}	Outlet water temperature of recovery loop	°C
T_{irec}	Inlet water temperature of recovery loop	°C
m_{rec}	Bypass flow	kg/s
HVAC	Heating Ventilation and Air Conditioning	-

1 Introduction

1.1 Background

Directive 2018/2001 / CE [1] has indicated to European countries a series of objectives related to energy efficiency and use of renewable energy, such as reduction of greenhouse gases by 20% and an increase in the contribution of renewable energy by 20% against total energy consumption. In recent years the gas heat pump has attracted much attention due to its environmentally friendly advantages and efficiency as well as energy savings [2,3]. Gas engine heat pumps (GEHP) are essentially the same as electric heat pumps (EHP). The difference is that in the GEHP the electric motor is replaced by an internal combustion engine based on an OTTO cycle. The advantage concerning for to the electric heat pump is the use of residual energy available for the production of domestic hot water or to prevent frost under extreme temperature conditions in winter. Accordingly, the result is not only a reduction of CO₂ emissions but also a reduction in energy consumption [4].

The main disadvantage of GEHP systems is the limited optimal zone of operation. Then, they require robust models for sizing with the variability of buildings energy needs. Besides, manufacturers have few different units, because they propose to use thermal energy storage, parallel installations and efficiency control systems to achieve high efficiency [5]. To ensure that GEHPs operate within the best economic zone, researchers propose combining GEHPs with hybrid power technology [6–9], energy storage technology [10,11], absorption heat pump [12] and photovoltaic integration [13–15]. These studies demonstrate the potential of these systems in combination with conventional installations. Therefore, it is necessary to develop new simulation models for analysing this technology in new simulation schemes. Simplified models will allow for optimal sizing of hybrid installations for heat and cold production. Therefore, it is required to have robust models for this technology that can be integrated into more complex simulation schemes.

Then, hybrid solutions could appear as solutions for distributed generation. Renewable gas contributes to the discharge and improvement of the air quality of our cities, and facilitate the energy transition towards a truly circular economy. Xiaofan et al. [9] got good economic and energetic results of hybrid power gas with thermal and electric energy storage. These authors [9] justified the need of suitable models to optimize control and operation of facilities. Recently, Qiang et al. [15] designed a novel system where GEHP is integrated with solar energy, energy storage and smart control of energy needs. Novel system [15] required an intelligent solution using a neural network to guarantee optimal operation. So, the proposal of this paper could be integrated into these complex algorithms [15–17] and will improve final results.

1.2 Thermal evaluation

Thermal models are necessary to enable evaluation of the corresponding energy behaviour. In this context, various models have been developed. These may be classified into two categories: detailed models or models based on balance equations and simplified models or models based on behaviour curves. Nonetheless, the main requirement for thermal characterization models is that it is easy to reproduce, and can be adapted for any system of gas engine heat pump.

From a review of reference literature, the use of balance equations to evaluate the performance of a GEHP is highlighted by analysis using energy and exergy balances on the complete unit [3,10], or each element of the system [6]. These studies shed light on the internal behaviour of these units and enable exergoeconomic analysis for decision making in environmental policy

definition algorithms, as shown in [18]. However, these require knowledge of internal operating data of the units not usually provided by manufacturers.

To solve the issue of lack of information on about internal operation parameters, researchers added mathematical components into physical models. This type of model is called hybrid models. Here are exemplary studies such as [19,20]. The first [19] proposes a set of corrective functions for the energy balances that characterise these machines. These functions are modified from experimental data employing an algorithm based on high complexity neural networks. However, the same author proposed a variant of this simplified model [21] with parameters set at typical values. Nevertheless, there has been no experimental validation for the validity of this hypothesis. The second study [20] coincided with the model typologies, but it offered an original proposal of how to integrate control of these units using a neural network.

These solutions have a high mathematical complexity, which is a disadvantage when integrated into simulation algorithms. Solving this limitation, simplifying the model and extrapolating it to other types of machines is a challenge to be solved. This problem is more pronounced when a multitude of heat, cold and electricity generation systems (with and without storage) are integrated into the same decision-making algorithm.

The most standard simulation tools for building air conditioning systems are TRNSYS [22] and EnergyPlus [23]. The proposal of these tools for simulation of GEHP systems is a routine based on a set of operating curves. These curves are obtained for a given unit and, valid hypotheses are generated for this technology. Additionally, TRNSYS [22], in corresponding TESS libraries, offers a TYPE for the detailed simulation of GEHP systems. This TYPE goes into the thermodynamic detail of the cooling cycle as well as the combustion stages of the engine. Thus, it requires the definition of a set of detail parameters, such as volumetric performance of the combustion chamber, cylinder size, etc. The main disadvantage of these models is the difficulty in defining the parameters necessary for their implementation. Most parameters are not provided in the manufacturer's data sheets and cannot be defined from the data available in them.

The use of simplified models or models based on behaviour curves let designers and engineers determine the energy performance of the system at different operating conditions. They have the advantage of a significantly reducing computational cost in comparison with detailed procedures. Instead, they require high experimentation of different units to demonstrate the validity of them.

Along this line, researchers have developed the characterisation of energy behaviour curves of the electric heat pump in relation to its thermal capacity, as well as the functional dependencies of the curves, with external climatic conditions, using water distribution temperature and partial load factor [24,25].

However, in some cases, authors use very simplified models due to the uncertainty existing in the real conditions of operation of the building. For example, Sheng et al. [26] studied the energy performance of GEHP using simulation tools. The authors used a simplified model, but they validated it using measurement from the real operation of buildings. Alternatively, Kamal et al. [27] who had an experimental installation with several GEHP units. Subsequently, these same authors [27] compared the results of the same with those obtained from a simulation in EnergyPlus [28] using the default model for GEHP system.

For the GEHP system, there are experimental modelling methods where thermal efficiency of the engine is established as a function of the corresponding torque and speed [16,29].

On the one hand, Bin Hu et al. [29] proposed a model to simulate gas driven heat pumps. The proposed methodology requires to know all technical details of these systems, for example, the expansion valve. However, manufacturers do not provide this information, and it is very difficult to approximate.

Also, QingkunMeng et al. [16] developed a mathematical model for optimizing the operation of engine and compressor. The model requires to be detailed and thanks to it, it is possible to optimize internal the operation parameters. However, it is not compatible to be integrated into building energy simulation algorithms.

Experimental studies such as [30,31] demonstrated dependencies on thermal behaviour of gas heat pump system with ambient air temperature, water temperature and partial load factor. These studies facilitate understanding of system behaviour. But, mathematical models are required to quantify them outside the range of experimental testing. This approach was not validated in these studies. Feng et al. [32] established detailed experimental results of the thermal behaviour of the motor coupled to these systems and the variations of the recoverable heat in it.

Additionally, studies such as [33] demonstrated the potential of the use of curves to establish optimal strategies for heat recovery. The results were based on experimental data and they were obtained using a detailed experimental facility. Furthermore, there are studies such as [34,35], where, based on experimental data, operating laws for a unit were obtained enabling evaluation in critical summer conditions [34] or combined with known demand [35]. Both of them [34,35] are useful to understand this technology and define the best experiments to analyse these units. Moreover, Fengguo et al. [12] experimentally demonstrated that it is possible to define optimal operating instructions for GEHP systems and, the importance of taking them into account in the design of this type of facilities.

Accordingly, experimental studies about GEHP have been well treated in the existing publications. Shah et al. [36] developed detailed studies about diesel engine driven heat pump, but they did not propose any model. Jiying et al. [37] who analysed the effect of renewable biogas as a fuel for GEHP system. Huanwei et al. [30] integrated evaporative cooling with GEHP system and studied energy performance in different operational conditions. Or, Liu et al. [35] who investigated the possibilities of these systems for the production of domestic heat water. Even, Mingtao et al. [38] defined an experimental facility where they tested different control strategies. Before this work, they used simulation [39] for studying GEHP system.

In the study presented here, the GEHP system behaviour curves are defined. Also, they allow to characterising the thermal behaviour of these systems in terms of thermal capacity, consumption and energy recovery, as well as the functional dependencies of the curves, on external climatic conditions, partial load factor and water distribution temperature. It is obtained using the experimental data. Besides, the model developed using this data, is valid for heating and cooling, and it is possible to be implemented in energy buildings performance simulation tools with control operation strategies.

Last, measurement and classification of energy efficiency of air conditioning systems, by regulations [40] and a multitude of research projects, is based on basic EER and COP indicators, or more sophisticated parameters such as SEER and SCOP [41]. Among recent publications, the

work of Alves et al. [42] where, under different climatic and operating conditions (partial load factor), performance variability of several models of electric heat pumps is evaluated. This study demonstrates the need to distinguish between nominal and average seasonal characteristics. Since results of instant characteristic sensitivity of machines are presented and how average seasonal performances of the same machine may be doubled according to operating conditions even more so in real buildings with variable operating conditions. Zhang et al. [43] showed the importance of the accumulation and the variations of operation of the buildings in the seasonal benefits of GEHP.

Proper evaluation of the seasonal performance of these systems may be problematic for designers due to the lack of precise data as regards the behaviour of heat pumps beyond nominal conditions. In fact, the majority of heat pump manufacturers still avoid providing detailed information concerning this point in their datasheets. Additionally, it is possible to obtain seasonal performance ratios using simulation tools, but models need to reflect the real performance of a commercial system with credible results.

1.3 Aims

Gas Engine Heat Pump requires simplified characterization models. These models allow evaluating its economic and energy impact independently. Alternately, they could be implemented in complex simulation algorithms for different commercial solutions with a low computational cost.

In the existing literature, there are detailed solutions with high mathematical complexity, which is a disadvantage when integrated into simulation algorithms. On the other hand, there are simplified models but whose main disadvantage is the difficulty in defining the parameters necessary for its implementation. Most of the parameters are not provided in the manufacturer's data sheets and cannot be defined from the data available in them.

Solving these limitations is a challenge to solve. In order to solve this gap in the existing literature of the technology, an inverse characterization methodology based on experimental measurements is carried out. For this purpose, the main manufacturers in the sector defined a sample of five units. This sample could be considered as a representation of the current state of the market for this technology.

The methodology carried out uses an experimental installation to analyze the different units tested under different operating conditions. With the results of the experimentation carried out, it will be possible to know the real thermal behaviour of these HVAC systems and to develop the simplified characterization model based on operating curves. These curves characterize the thermal behaviour of these systems in terms of thermal capacity, energy consumption and recovery, as well as the functional dependencies of the curves, in external climatic conditions, partial load factor and water distribution temperature using experimental data provided by the manufacturers. Therefore, experimental results and proposed curves are the most relevant findings of this work.

The defined curves allow evaluating the thermal behaviour of these systems under any operating condition of the GEHP system and based on parameters available in the manufacturer datasheets. This developed model is valid for heating and cooling. Also it can be implemented in performance simulation tools of energy buildings with control operation strategies. Then, usability and replicability of this work is can be high.

The proposed model is highly accurate and easy to reproduce. The results of the validation performed show a maximum error of 25% and an average error of less than 7%.

2 Characterization of the gas heat pump system

2.1 Basic operation of GEHP systems

Gas Heat Pumps (GEHP) are essentially the same as electric heat pumps (EHP), based on a thermodynamic cycle in which energy is transferred from a cold source to a hot source by application through the compressor shaft of the equipment. Its difference is that in the GEHP, the electric motor coupled to the compressor in the electric heat pump is replaced by an internal combustion engine based on an OTTO cycle.

This engine is fed with fossil gas fuel and must be cooled to remove the residual heat generated during operation. The heat generated from cooling the engine block, the oil pan and exhaust gases are transmitted to a hydraulic circuit to be used to produce hot water. This hot water is produced from residual heat. Additionally, when external temperatures are excessively low, this heat is used to prevent the formation of frost on the evaporator without the need for cycle inversion. This functionality enables excellent performance from this type of machine at low temperatures. Fig. 1 displays a schematic view of a gas engine heat pump (system) in cooling mode.

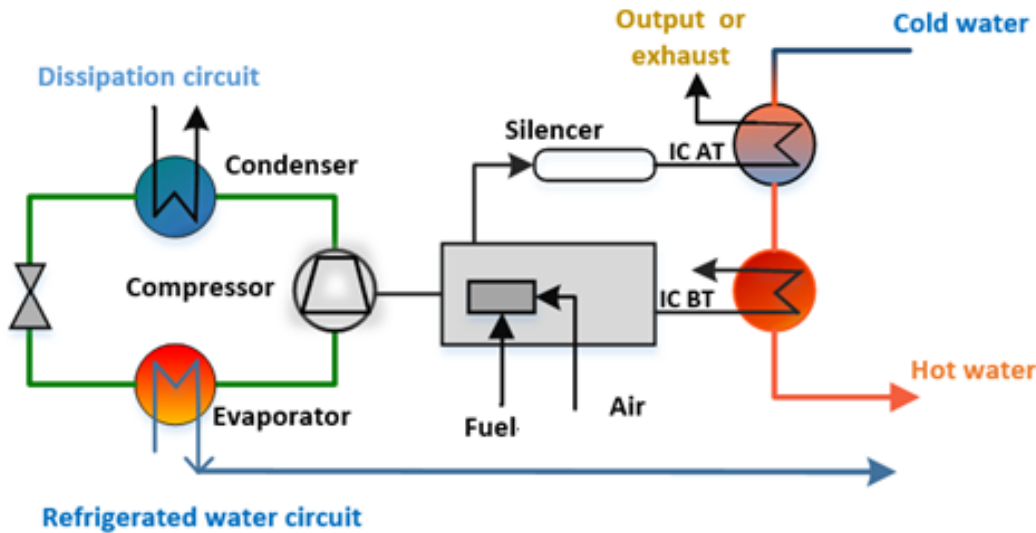


Figure 1. Schematic diagram of a GEHP cycle in cooling mode

The right part of figure 1 demonstrates how the machine combustion engine consumes fuel and air to drive the compressor of the heat pump. Cooling the engine (see IC BT in figure 1), totally or partially, heat is recovered in the form of hot water; the remaining, if any, is evacuated to the exterior. Besides, heat of exhaust gas is recovered (see IC AT in figure 1). If the left part of Figure 1 is analysed, the compression cycle of the system may be observed. In Figure 1, operation in cooling mode is schematised. In this mode, the heat pump produces cold water in the evaporator and heat dissipates in the condenser with the outside environment. The heating mode is achieved by inverting the compression cycle on the left, as with conventional heat pumps. Control of the machine is carried out on the rotational speed of the compressor, i.e., by controlling the combustion engine.

GEHP systems are equipped with a 4-stroke engine and 3 or 4 cylinders in line, which moves between 952-1998 cm³ rotating between 600 and 3000 rpm, depending on model, brand and load. These motors rotate, employing a belt system, depending on the model, one or two open scroll compressors. The management system of these motor-compressor assemblies decides their optimum speed of rotation and eventually, the partial load ratio of the compressors. These decisions depend on the needs in order to achieve maximum energy efficiency at all times, especially at partial loads.

It should be noted that there are developments of two types of machines: hydronic systems that produce cold or hot water to compensate for the demands of cooling and heating respectively, and direct expansion systems. The latter pushes coolant in a gaseous state under different pressure conditions for producing cold or heat in conditioned areas. This study focuses on hydronic systems.

2.2 Assumptions

The proposed methodology aims to analyze and characterize GEHP systems through experimental data. For this, detailed experiments have been carried out on different machines, and a characterization model based on operating curves has been developed. The assumptions considered in the development of this work after analysis of the technology and pooling with manufacturers are the following:

- Operation is considered at a constant water flow rate (m_w), i.e., the heat pump operates by varying the T_{ow} output temperature of the fluid streams with which it exchanges heat.
- A gas internal combustion engine drives these machines. Their operation is carried out with modulation between load levels (PLR): stopped (0%), half load (50%) and full load (100%).
Therefore, a possible maximum and minimum load level has been established.
- The minimum load ratio is 30% according to manufacturers, with a maximum of 130%.
- The maximum heat production temperature in the condenser is 55°C. The minimum evaporator output temperature is 4°C and the maximum recovery water temperature may reach 65°C.
- 7°C is used as the minimum outside air temperature for recovery of residual heat from the engine ($T_{lim-rec}$). Recovery is not possible at lower temperatures.
- The heat pump can operate producing heat for heating, DHW and cold water for cooling; depending on the established set-point temperature ($T_{setpoint}$). Additionally, hot water will be generated from residual heat generated during engine cooling ($Q_{recovery}$).
- The heat to be evacuated with the environment is carried out by air-coolers, from which ventilator consumption is calculated.

The following sections describe the basis of the model and its formulation.

2.3 Description of the system characterisation

Characterisation of the GEHP system is based on behavioural equations obtained from experimental data. Besides, algorithm contains the sequence of required operations and decisions regarding internal control.

This study adopts a computation approach for modelling the GEHP system and the installations. Following the modelling philosophy, the system variables may be classified into three types:

parameters, inputs and outputs. The following diagram displays the direction of these variables for system characterisation.

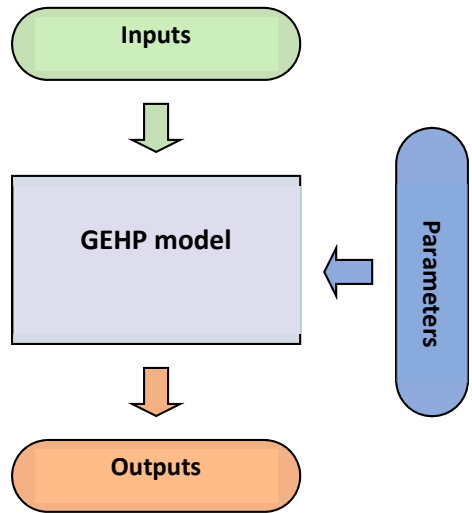


Figure 2. Modelling philosophy

The set of variables that comprise part of the definition of the GEHP system and remain unchanged during simulation are called parameters. These parameters are supplied at the beginning of the simulation and remain constant during the simulation. Parameters generally represent dimensions, nominal powers, operating curves and constructive, geometric and thermal characteristics of the different elements. They may also represent operating limits or any other type of equipment constraint.

The existence of independent variable terms during the simulation (inputs) is mainly due to two causes:

- Variation due to the moment being analysed. This group includes energy demand, outdoor temperature, solar radiation, etc.
- Dynamic effect such as temperatures and flow rates of the different operating fluids.

Independent variables generate a set of inputs and must be provided to the units during each simulation interval.

Once the parameters and inputs are known, characterisation of the system that identifies the unit may be resolved. The result of this calculation generates a set of outputs. Given that every system is comprised of interconnected elements, the outputs of each unit constitute the inputs of subsequent units.

As previously mentioned, system characterisation integrates a set of curves that enable calculation of the real performance of the GEHP system. These curves characterise the thermal behaviour of these systems in terms of thermal capacity, consumption (electric and gas) and energy recovery based on the variation of operating and climatic conditions concerning the nominal data indicated in manufacturer's catalogues. Curve coefficients are obtained from data extracted from experiments and would appear as algorithm parameters. All details as regards formulation and collection are explained in section 2.4 "Experimental performance curves".

Table 1 displays the system input variables.

Table 1. Inputs of the proposed system characterisation

Description	Units
Inlet temperature of water	°C
Water flow in GEHP	kg/s
Setpoint for GEHP	°C
Outdoor dry-bulb temperature	°C
Outdoor web-bulb temperature	°C
Set partial load ratio	%
Inlet water temperature in recovery loop	°C
Water flow in recovery loop	kg/s
Operation mode	1 heating, 2 cooling, 3 domestic hot water, 0 off

Input variables (see table 1) may be classified into those referring to the characterisation of water flows entering the system (heating / cooling and recovery water flows) employing temperature and flow rate; exterior conditions; and control signals referring to regulation type and operation mode. Conversely, table 2 shows the parameters of the system definition.

Table 2. Parameters of the proposed system characterization

Description	Units
Heat capacity	kW
Cooling capacity	kW
Gas consumption in heating mode by the engine	kW
Gas consumption in cooling mode by the engine	kW
Electricity consumption in heating mode	kW
Electricity consumption in cooling mode	kW
Recovery heat for domestic hot water	1 yes, 0 no
Nominal capacity of heat recovery	kW
Maximum temperature of hot water production	°C
Minimum temperature of cold water production	°C
Maximum temperature of recovery loop	°C
Minimum partial load ratio	%
Maximum partial load ratio	%
Coefficients of performance curves	Section 2.4

Finally, calculated outputs are detailed in table 3.

Table 3. Outputs of the proposed system characterization

Description	Units
Outlet water temperature of GEHP	°C
Outlet water temperature of recovery loop	°C
Gas consumption	kW
Electricity consumption	kW
Heat production of GEHP for heating	kW
Cooling production of GEHP for cooling	kW
Recovery heat of engine	kW

Description	Units
Operation partial load ratio	%
Efficiency of GEHP (heating in condenser or cooling in evaporator)	-
Efficiency of the system: GEHP + Recovery	-

The system outputs (see table 3) display the characterisation variables of water flows from the machine's outlet (condenser/evaporator and recovery in the gas engine); energy flows exchanged for heating, cooling and DHW; fuel consumption; partial load factor and operating performance.

2.4 Experimental performance curves

System characterisation integrates a set of curves that enable calculation of the real performance of the GEHP system. These curves characterise the thermal behaviour of these systems in terms of thermal capacity, consumption (electricity and gas) and energy recovery based on the variation of operating and climatic conditions concerning the nominal data indicated in manufacturer's catalogues. In other words, the value of a given variable in real conditions shall be given by the product of its nominal value and the value of the corresponding behaviour curve in these conditions, according to Eq. 1:

$$\text{Real value} = \text{Performance curve} \cdot \text{Nominal value} \quad \text{Eq. (1)}$$

Behaviour curves obtained for this system may be classified according to whether they contain one or two independent variables. Below (Table 4) describes the different types of curves for these two categories. (formulation of curves is the most common in software like DOE2-2 [44] or TRNSYS [22])

Table 4. Behaviour curve typology

Form	Equation
Quadratic	$f(r) = a + b \cdot r + c \cdot r^2$
Cubic	$f(r) = a + b \cdot r + c \cdot r^2 + d \cdot r^3$
bi-quadratic	$f(r_1, r_2) = a + b \cdot r_1 + c \cdot r_1^2 + d \cdot r_2 + e \cdot r_2^2 + f \cdot r_1 \cdot r_2$

Table 5 describes the general formulation of the different behaviour curves, as well as their dependencies. r , r_1 and r_2 are dependent variables and a , b , c , d , e , f are the coefficients of the curves. The criteria adopted to choose in function of the involved parameter is the best interpolating curve. To obtain the coefficients of each of the curves displayed in said table, the following is carried out:

- 1- Extraction of data from the experiment where the variable in question appears with the respective dependencies.
- 2- The normalisation of the values under different operating conditions with respect to nominal conditions (Eq. 2).
- 3- Determination of adjustment coefficients for the equation type indicated in Table 3 (Form)

$$\text{Normalized variable} = \frac{\text{Experimental value of variable}}{\text{Nominal value of variable}} \quad \text{Eq. (2)}$$

Table 5. Description and dependencies of behaviour curves

Name	Form	Description	Independent Variables
------	------	-------------	-----------------------

COOLCAPT	bi-quadratic	Variation of cooling capacity (PLR=100%) as a function of outlet water temperature and outdoor dry-bulb temperature	$f(T_{ow}, T_{dr})$
HEATCAPT	bi-quadratic	Variation of heating capacity (PLR=100%) as a function of outlet water temperature and outdoor wet-bulb temperature	$f(T_{ow}, T_{wb})$
COLDCONT	bi-quadratic	Variation of gas consumption in cooling mode (PLR=100%) as a function of outlet water temperature and outdoor dry-bulb temperature	$f(T_{ow}, T_{dr})$
COLDCONPLR	cubic	Variation of gas consumption in cooling mode as a function of partial load ratio	$f(PLR)$
HEATCONT	bi-quadratic	Variation of gas consumption in heating mode (PLR=100%) as a function of outlet water temperature and outdoor wet-bulb temperature	$f(T_{ow}, T_{wb})$
HEATCONPLR	cubic	Variation of gas consumption in heating mode as a function of partial load ratio	$f(PLR)$
RECCOLDCAPT	bi-quadratic	Variation of heat recovery in cooling mode (PLR=100%) as a function of outlet water temperature and outdoor dry-bulb temperature	$f(T_{ow}, T_{dr})$
RECCOLDCAPPLR	cubic	Variation of heat recovery in cooling mode as a function of partial load ratio	$f(PLR)$
RECHEATCAPT	bi-quadratic	Variation of recovery heat in heating mode (PLR=100%) as a function of outlet water temperature and outdoor wet-bulb temperature	$f(T_{ow}, T_{dr})$
RECHEATCAPPLR	cubic	Variation of heat recovery in heating mode as a function of partial load ratio	$f(PLR)$
COLDECONT	quadratic	Variation of electricity consumption in cooling mode (PLR = 100%) as a function of outdoor dry-bulb temperature	$f(T_{dr})$
COLDCONPLR	cubic	Variation of electricity consumption in cooling mode as a function of partial load ratio	$f(PLR)$
HEATECONT	quadratic	Variation of electricity consumption in heating mode (PLR = 100%) as a function of outdoor wet-bulb temperature	$f(T_{wb})$
HEATECONPLR	cubic	Variation of electricity consumption in heating mode as a function of partial load ratio	$f(PLR)$

Additionally, generic curves are defined for each type described in Table 5. These generic curves adjusted using the total set of experimental data available allow that the model proposed can be executed for any system of the gas engine heat pump. The adjustment coefficients of all types of curves for the five available units and the generic unit are shown in APPENDIX "Operation Curves".

2.5 Gas heat pump algorithm

The diagram represented in figure 1 outlines the proposed calculation sequence. The following details each of the steps carried out.

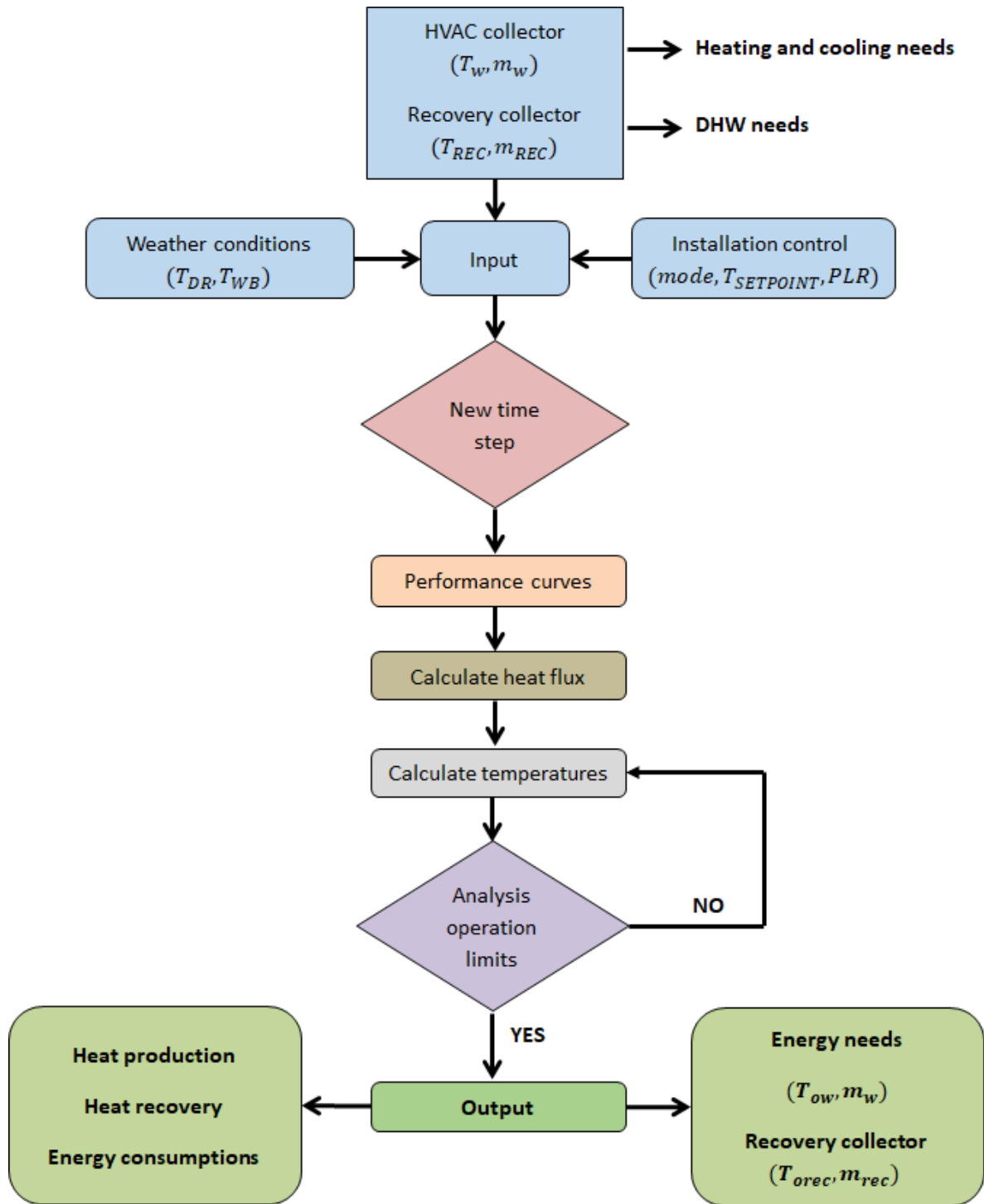


Figure 3. Calculation procedure implemented in TRNSYS

The internal operations of the machine depend on the operation mode. The operation mode may be heating (operation mode = 1), cooling (operation mode = 2) or domestic hot water (DHW) (operation mode = 3).

The main highlights of the algorithm are summarised in the following lines. It should be noted that the guidelines, are not indicated, instead only the steps executed to quantify heat fluxes and to calculate temperatures:

1. Comparison of water inlet temperature, T_{IW} , with the desired set-point temperature. If the temperature difference is less than 0.5°C , the machine will not operate, and the input conditions with no consumption are returned as outputs.

As well, if in heating or DHW mode the inlet temperature is higher than the set-point, the unit will not operate. Something similar to what occurs during cooling, if the inlet temperature is lower than the established set-point. Finally, if the inlet temperature of the recovery circuit is higher than the maximum allowed, the residual heat of the engine is evacuated and heat is not transferred to the recovery circuit.

2. Once partial load factor, PLR, and flow temperature T_{SETPOINT} are established; with exterior conditions for heat exchange with the environment known, the operating curve calculation is carried out. These curves enable estimation of heat fluxes in real operating conditions of the unit as a function of nominal conditions.

Production of hot water in heat pump (Mode=1 or 3)

The heat flux delivered by the condenser is calculated using equation 3:

$$Heat_{real}[kW] = PLR \cdot HEATCAPT \cdot Heat_{nom}[kW] \quad \text{Eq. (3)}$$

Where $Heat_{real}[kW]$ is heat capacity in real operation conditions, $Heat_{nom}[kW]$ is heat capacity in nominal operation conditions, and HEATCAPT is the variation of heating capacity (PLR=100%) as a function of outlet water temperature and outdoor wet-bulb temperature. PLR is defined as the quotient between the energy delivered by the machine $Heat_{real}[kW]$ and its nominal capacity $Heat_{nom}[kW]$.

Likewise, gas consumption of the engine and electric system is calculated according to equations 4 and 5:

$$ConGasH_{real}[kW] = HEATCONPLR \cdot HEATCONT \cdot ConGasH_{nom}[kW] \quad \text{Eq. (4)}$$

Where $ConGasH_{real}[kW]$ is gas consumption in heating mode in real operation conditions, $ConGasH_{nom}[kW]$ is gas consumption in heating mode in nominal operation conditions, HEATCONPLR is variation of gas consumption in heating mode as a function of partial load ratio and HEATCONT is variation of gas consumption in heating mode (PLR=100%) as a function of outlet water temperature and outdoor web-bulb temperature.

$$ConElecH_{real}[kW] = HEATECONPLR \cdot HEATECONT \cdot ConElecH_{nom}[kW] \quad \text{Eq. (5)}$$

Where $ConElecH_{real}[kW]$ is electrical consumption in heating mode in real operation conditions, $ConElecH_{nom}[kW]$ is electrical consumption in heating mode in nominal operation conditions, HEATECONPLR is variation of electricity consumption in heating mode as a function of partial load ratio and HEATECONT is variation of electricity consumption in heating mode (PLR = 100%) as a function of outdoor wet-bulb temperature.

Finally, recoverable heat in the engine is estimated using equation 6:

$$RecQH_{real}[kW] = RECHEATCAPPLR \cdot RECHEATCAPT \cdot RecQH_{nom}[kW] \quad \text{Eq. (6)}$$

Where $RecQH_{real}[kW]$ is heat recoverable in heating mode in real operation conditions, $RecQH_{nom}[kW]$ is heat recoverable in heating mode in nominal operation conditions, RECHEATCAPPLR is variation of heat recovery in heating mode as a function of partial load ratio and RECHEATCAPT is variation of recovery heat in heating mode (PLR=100%) as a function of outlet water temperature and outdoor web-bulb temperature.

It should be noted that the calculated energy flows relate to the desired operating conditions. In point 3 (equations 11 and 12), the corresponding outlet temperatures are calculated and analysed if valid within the operating limits of the machine.

Production of cold water in heat pump (Mode=2)

Cooling mode treatment is analogous to heating mode. Equation 7 enables estimation of cooling power, equations 8 and 9 estimate energy consumption of the machine; and finally equation 10 is equivalent to equation 4 but uses the behaviour curves of the machine in cold mode to estimate recoverable heat:

$$Cold_{real}[kW] = PLR \cdot COLDCAPT \cdot Cold_{nom}[kW] \quad \text{Eq. (7)}$$

Where $Cold_{real}[kW]$ is cooling capacity in real operation conditions, $Cold_{nom}[kW]$ is cooling capacity in nominal operation conditions, COLDCAPT is variation of cooling capacity (PLR=100%) as a function of outlet water temperature and outdoor wet-bulb temperature and PLR is defined as the quotient between the energy delivered by the machine $Cold_{real}[kW]$ and its nominal capacity $Cold_{nom}[kW]$.

$$ConGasC_{real}[kW] = COLDCONPLR \cdot COLDCONT \cdot ConGasC_{nom}[kW] \quad \text{Eq. (8)}$$

Where $ConGasC_{real}[kW]$ is gas consumption in cooling mode in real operation conditions, $ConGasC_{nom}[kW]$ is gas consumption in cooling mode in nominal operation conditions, COLDCONPLR is variation of gas consumption in cooling mode as a function of partial load ratio and COLDCONT is variation of gas consumption in cooling mode (PLR=100%) as a function of outlet water temperature and outdoor web-bulb temperature.

$$ConElecC_{real}[kW] = COLDECONPLR \cdot COLDECONT \cdot ConElecC_{nom}[kW] \quad \text{Eq. (9)}$$

Where $ConElecH_{real}[kW]$ is the electricity energy consumption in heating mode in real operation conditions, $ConElecH_{nom}[kW]$ is the electricity energy consumption in heating mode in nominal operation conditions, HEATECONPLR is the variation of electricity consumption in heating mode as a function of partial load ratio and HEATECONT is the variation of electricity consumption in heating mode (PLR = 100%) as a function of outdoor wet-bulb temperature.

$$RecQC_{real}[kW] = RECCOLDPLR \cdot RECCOLDT \cdot RecQC_{nom}[kW] \quad \text{Eq. (10)}$$

Where $RecQC_{real}[kW]$ is heat recoverable in cooling mode in real operation conditions, $RecQC_{nom}[kW]$ is heat recoverable in cooling mode in nominal operation conditions, RECCOLDPLR is the variation of heat recovery in cooling mode as a function of partial load ratio and RECCOLDAPT is the variation of recovery heat in cooling mode (PLR=100%) as a function of outlet water temperature and outdoor web-bulb temperature.

3. Output flow temperatures are eliminated from heat fluxes:

Production of hot water in heat pump (Mode=1 or 3)

In heating mode, the water comes out hotter from both the condenser (equation 11) and the heat recovery circuit of the engine (equation 12):

$$T_{ow}[^{\circ}C] = \frac{Heat_{real}[kW]}{Cp_W \left[\frac{kJ}{kg \cdot K} \right] \cdot m_W \left[\frac{kg}{s} \right]} + T_{iw} \quad \text{Eq. (11)}$$

T_{ow} is condenser outlet water temperature, T_{iw} is condenser inlet water temperature, $Heat_{real}$ is heat capacity in real operation conditions, Cp_W is specific heat of water and m_W is condenser water flow.

$$T_{orec}[^{\circ}\text{C}] = \frac{RecQH_{real}[\text{kW}]}{Cp_W[\frac{\text{kJ}}{\text{kg}\cdot\text{K}}] \cdot m_{rec}[\frac{\text{kg}}{\text{s}}]} + T_{irec} \quad \text{Eq. (12)}$$

T_{orec} is outlet water temperature of recovery loop, T_{irec} is inlet water temperature of recovery loop, $RecQH_{real}$ is heat recoverable in heating mode in real operation conditions, Cp_W is specific heat of water and m_W is recovery circuit water flow.

Production of cold water in heat pump (Mode=2)

Conversely, in cooling mode the water is cooled in the evaporator according to equation 13 and the heated water temperature in the recovery circuit according to equation 14:

$$T_{ow}[^{\circ}\text{C}] = T_{iw} - \frac{Cold_{real}[\text{kW}]}{Cp_W[\frac{\text{kJ}}{\text{kg}\cdot\text{K}}] \cdot m_W[\frac{\text{kg}}{\text{s}}]} \quad \text{Eq. (13)}$$

T_{ow} is condenser outlet water temperature, T_{iw} is condenser inlet water temperature, $Cold_{real}$ is cooling capacity in real operation conditions, Cp_W is specific heat of water and m_W is condenser water flow.

$$T_{orec}[^{\circ}\text{C}] = \frac{RecQC_{real}[\text{kW}]}{Cp_W[\frac{\text{kJ}}{\text{kg}\cdot\text{K}}] \cdot m_{rec}[\frac{\text{kg}}{\text{s}}]} + T_{irec} \quad \text{Eq. (14)}$$

T_{orec} is recovery circuit outlet water temperature, T_{irec} is recovery circuit inlet water temperature, $RecQC_{real}$ is heat recoverable in cooling mode in real operation conditions, Cp_W is specific heat of water and m_W is recovery circuit water flow.

Accordingly, the calculated temperatures referenced the expected values according to previously estimated flows and desired operating conditions. However, in Table 2, the machine parameters are defined, where the operating limits are indicated. If the water flow temperature calculated with equation 11 (heating mode) or 12 (cooling mode) is out of limits, an iterative process is carried out to establish a suitable partial load factor close to that desired. Moreover, the recovery temperature calculated with equations 13 and 14 cannot exceed a maximum value. Otherwise, the maximum value would be established, and the remaining recoverable heat would dissipate.

4. Finally, once the heat fluxes are known and the desired, valid operating conditions are established according to the iterative process. Then the efficiency indicators can be calculated. These indicators may be divided into two groups, those referencing the system cooling cycle (COP equation 15 and EER equation 16); and those referencing the entire system (COP_{SYSTEM} equation 17 and EER_{SYSTEM} equation 18):

$$COP = \frac{Heat_{real}[\text{kW}]}{ConGasH_{real}[\text{kW}]} \quad \text{Eq. (15)}$$

$Heat_{real}$ is heat capacity in real operation conditions, and $ConGasH_{real}$ is gas consumption in heating mode in real operation conditions.

$$EER = \frac{Cold_{real}[\text{kW}]}{ConGasC_{real}[\text{kW}]} \quad \text{Eq. (16)}$$

$Cold_{real}$ is cooling capacity in real operation conditions, and $ConGasC_{real}$ is gas consumption in cooling mode in real operation conditions.

If the entire system is considered, the numerator must be added to the heat flux recovered in the engine. In such a way that the returns calculated with equations 17 and 18 are higher than those estimated with equations 15 and 16:

$$COP_{SYSTEM} = \frac{Heat_{real}[kW] + RecQH_{real}[kW]}{ConGasH_{real}[kW]} \quad \text{Eq. (17)}$$

$Heat_{real}$ is heat capacity in real operation conditions, $RecQH_{real}$ is heat recoverable in heating mode in real operation conditions and $ConGasH_{real}$ is gas consumption in heating mode in real operation conditions.

$$EER_{SYSTEM} = \frac{Cold_{real}[kW] + RecQC_{real}[kW]}{ConGasC_{real}[kW]} \quad \text{Eq. (18)}$$

$Cold_{real}$ is cooling capacity in real operation conditions, $RecQH_{real}$ is heat recoverable in cooling mode in real operation conditions and $ConGas_{real}$ is gas consumption in cooling mode in real operation conditions.

The GEHP operation depends on the partial load factor (PLR, namely partial load ratio) and in this paper, it refers to PLR as the ratio between the actual power transferred by the GEHP and the maximum power (see equation 3). The latter is the definition of the capacity ratio (CR), more useful to use when the interaction between plant and building has to be determined for evaluation of real operation conditions. Indeed, it represents one of the relevant parameters to consider for the correct identification of the operational curves.

3 Results

3.1 Experimental facility

Two manufacturers of this technology have collaborated in the development and validation of the results indicated: Panasonic and Aisin. These manufacturers have selected several of their commercial models, and have collaborated to carry out the operational experiments in climatic chambers. These tests are used in many applications related to the experimental analysis of construction elements or equipment [45–47]. Testing consists of generating a chamber with controlled temperature and humidity conditions. The experiment consisted of the assembly of the installation presented in Figure 4.

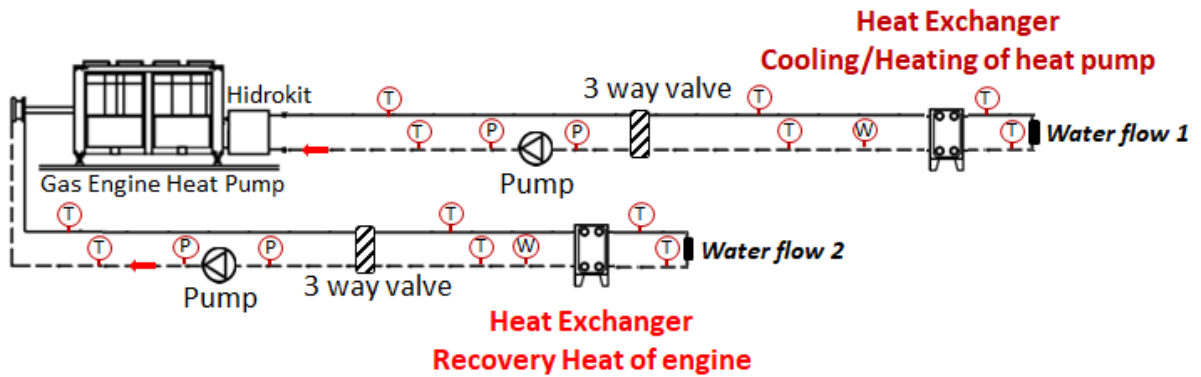


Figure 4. Schematic diagram of the experimental setup

Figure 4 shows a schematic position of sensors. There is three type of monitors: temperature [T], pressure [P] and water flow [W]. Sensor of temperature is a thin film platinum resistor - Pt100 - trimmed at a laboratory to comply with the resistance values of the standard IEC 60751, class A (error less than 1%). The pressure sensor is a 1/4"NPT Pressure Gauge Pressure Manometer (Hydraulic Gauge 0-4 Bar 0-60 PSI). Water flow sensor is a high-accuracy [0.2 % ±1 mm/s] mass flow measurement [measuring range 0 to 10 m/s].

Installation of Figure 4 enables:

- Real-time data results in every 60 s for water temperatures, flow rates and pressures for the most representative points of the installation. Sampling has been carried out within a short period time to ensure stabilised measurements.
- Control of the GEHP unit operating parameters: heat/cold flows, recovery mode and load of the engine.
- Generation of heat and cold loads in water flow 1 (heating and cooling). Maintenance of constant heat flux 2 temperature for heat recovery.
- Control of return temperature of water flows entering the machine.

On the other hand, it is interesting to note that the experimental installation has an estimated cost of more than 40000€ (not including the price of GEHP systems and climatic chambers).

Accordingly, two types of experiments are carried out. Type 1 experiment consists of a full load operation of the engine, maintaining the water return temperature constant while varying the environmental conditions and flow temperature. Type 2 experiment consists of maintaining the environmental conditions and flow temperature constant, in order to vary the workload of the engine. These experiments are carried out under different conditions until obtaining the functional maps of the machines.

It has been used five machines from different manufacturers. Table 6 and 7 show datasheet of the tested units. This sample represents the most usually units in the market since these manufactures.

Table 6. Studied GEHP units: nominal parameters of heating

ID	List of GEHP units	Capacity [kW]	Nominal conditions: heating mode			
			Gas consumption [kW]	Electricity consumption [kW]	COP	Recovery heat [kW]
1	Panasonic ECO-g with Hidrokit (U-20GE2E5 + S-500WX2E5)	60	42.5	0.65	1.48	20
2	Panasonic ECO-g with Hidrokit (U-30GE2E5 + S-710WX2E5)	80	68.1	1.46	1.40	30
3	AISIN AXGP450E1-16HP + AWS 16HP-E1(J) P450	47.5	30.2	1.24	1.58	16.5
4	AISIN AXGP560E1-20HP + AWS 20HP-E1(J) P560	60	42	1.24	1.50	20
5	AISIN AXGP710E1-25HP + AWS 25HP-E1(J) P710	75	53.6	1.4	1.49	25

Table 7. Studied GEHP units: nominal parameters of cooling

ID	List of GEHP units	Capacity [kW]	Nominal conditions: cooling mode			
			Gas consumption [kW]	Electricity consumption [kW]	EER	Recovery heat [kW]
1	Panasonic ECO-g with Hidrokit (U-20GE2E5 + S-500WX2E5)	50	39.1	1.03	1.43	20
2	Panasonic ECO-g with Hidrokit (U-30GE2E5 + S-710WX2E5)	71	67.9	1.71	1.25	30

3	AISIN AXGP450E1-16HP with AWS 16HP-E1(J) P450	41	32	1.28	1.45	16.5
4	AISIN AXGP560E1-20HP with AWS 20HP-E1(J) P560	52	41.5	1.32	1.38	20
5	AISIN AXGP710E1-25HP with AWS 25HP-E1(J) P710	63	55.1	1.59	1.29	25

It is important to note that the nominal recoverable heat for DHW production is identical in both operation modes due to being linked to the internal combustion engine.

3.2 Experimental results

This section describes the experimental data obtained according to the details summarised in section 3.1. The different experiments carried out are summarized in Table 8 and Table 9.

Table 8. Experiment of heating mode: organization

WATER SYSTEM HEATING MODE			Dry-bulb temperature (°C)						
			-10	-5	0	5	10	15	20
Water Temperature (inlet-outlet)	°C	30-35	File 1	File 2	File 3	File 4	File 5	File 6	File 7
		40-45	File 8	File 9	File 10	File 11	File 12	File 13	File 14

Table 9. Experiment of cooling mode: organization

WATER SYSTEM COOLING MODE			Dry-bulb temperature (°C)							
			0	10	20	25	30	35	40	45
Water Temperature (inlet-outlet)	°C	12 - 7	File 15	File 16	File 17	File 18	File 19	File 20	File 21	File 22
		23 - 18	File 23	File 24	File 25	File 26	File 27	File 28	File 29	File 30

The parameters chosen to perform the experiments in table 8 and **¡Error! No se encuentra el origen de la referencia.** have been established with the manufacturers. The environmental conditions used analyse the minimum and maximum expected temperatures in the climatic regions of the Mediterranean [48]. Furthermore, flow temperatures in heating mode (Table 8) are 35°C and 45°C, which indicate a low flow temperature. However, these machines may reach temperatures of 55°C - 60°C in the condenser flow with a poor performance [35]. On the other hand, in cold mode (table 9) operation is outlined under usual flow conditions at 7°C and a return at 12°C, with a high flow temperature of 18°C. This second alternative is designed so that the GEHP system works as a base in a conventional air conditioning scheme, for example, for pre-treatment of ventilation air.

Table 10 shows the variation of machine performance for a constant flow temperature, two different environmental conditions, and a partial load factor varying between 30% to 100%. Data of Table 10 is corresponding with experiment of file 10 (Table 10)

Table 10. Experiment of cooling mode: example file 18

Unit ID	Mode	Water Outlet T / Indoor T [°C]	Outdoor T [°C]	Load [%]	Capacity [kW]	Gas Consumption [kW-LHV]	Electricity Consumption [kW]	Engine heat recovery [kW]	COP/EER [Capacity / Gas consumption]	Specific Engine heat recovery [Heat recovery / Gas consumption]
---------	------	--------------------------------	----------------	----------	---------------	--------------------------	------------------------------	---------------------------	--------------------------------------	---

3	Cool	7	25	30	14.7	7.2	0.1	3.6	2.04	0.51
3	Cool	7	25	40	17.3	8.8	0.2	4.4	1.97	0.51
3	Cool	7	25	50	21.9	11.9	0.2	6.0	1.84	0.50
3	Cool	7	25	60	26.5	15.1	0.3	7.6	1.75	0.50
3	Cool	7	25	70	31.0	18.2	0.4	9.1	1.70	0.50
3	Cool	7	25	80	35.2	21.1	0.4	10.6	1.67	0.49
3	Cool	7	25	90	39.5	24.1	0.5	12.1	1.64	0.49
3	Cool	7	25	100	44.0	27.2	0.5	13.6	1.62	0.49

However, the wealth of experimental data available enables detailed analysis. Given that the measurements indicated in the table are obtained when the machine reaches a stationary operating regime for given conditions.

As an example of the experimental results obtained, the behaviour of the Panasonic machine U20 (ID 1, table 3 and table 4) is displayed in Figure 5 and Figure 6. Figure 5 displays the operation in heating mode (production of hot water in the condenser) at 100% load and for two flow temperatures (35°C and 45°C).

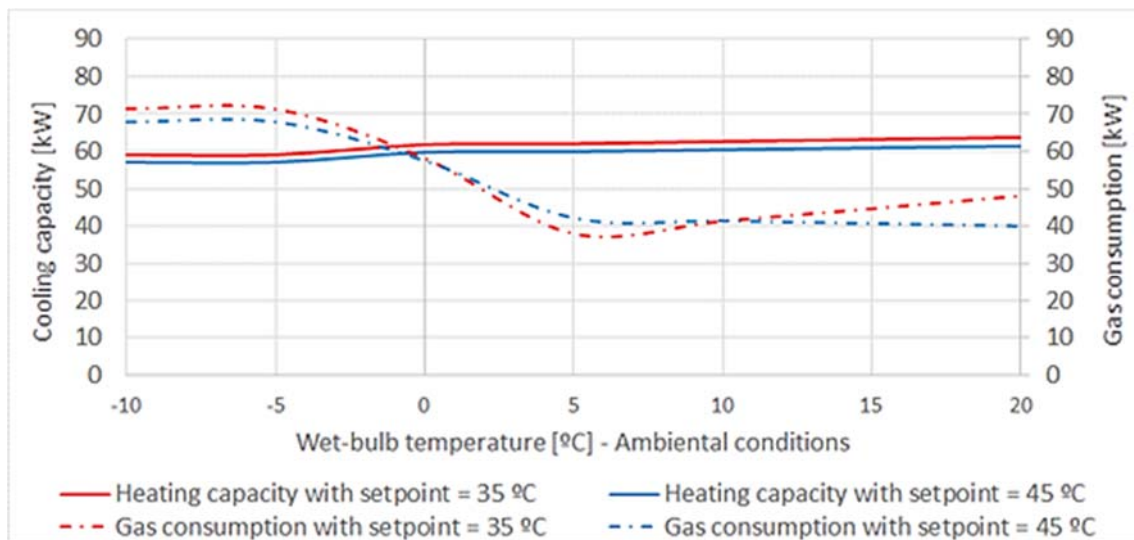


Figure 5. Analysis of Unit ID 1: influence of set-point in heating mode

Figure 5 shows that although heat generation in the cycle condenser is stable with the temperature operating at 100%, gas consumption is affected. This is because the behaviour of the gas engine worsens at low temperatures [35]; even manufacturers recommend that these machines not be operated when the outdoor dry temperature is below -5°C.

In Figure 6, the experimental results are displayed for the same machine studied in Figure 5, but in cooling mode (production of cold water in the evaporator). As in the previous case (Figure 5), the experiments are carried out at 100% engine load and at two flow temperatures (7°C and 18°C).

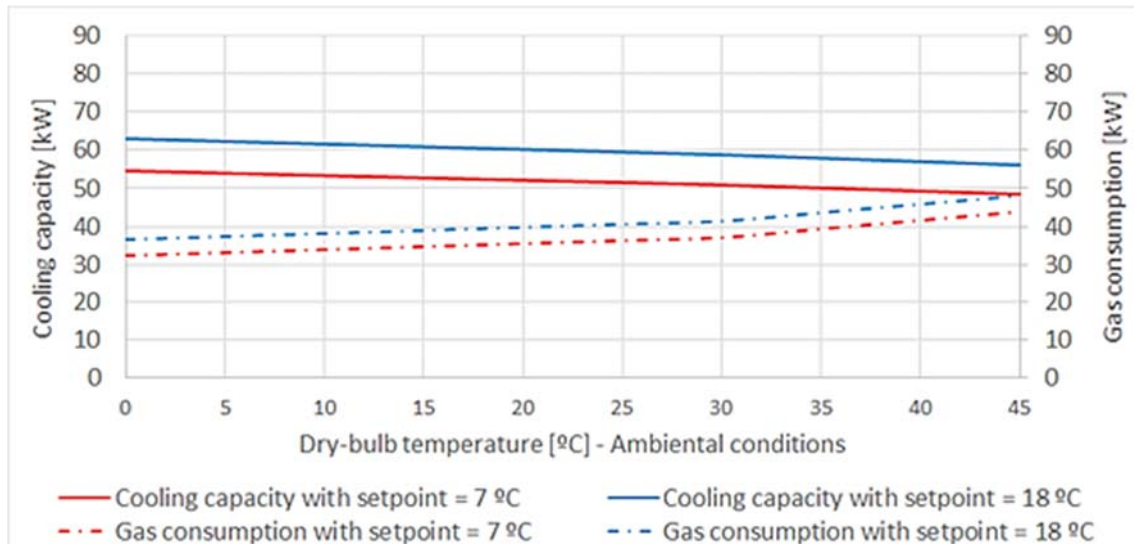


Figure 6. Analysis of Unit ID 1: influence of set-point in cooling mode

The results displayed in Figure 6 are stable. The higher the flow temperature in the evaporator, the better the performance, as is postulated in Carnot's theorem [49]. However, as the outdoor temperature increases, it is more difficult for the condenser to dissipate the heat, lowering the performance of the cooling cycle, thus lowering the cooling capacity to 100% of the engine. Likewise, for the engine to maintain the operating range, it must increase its consumption to ensure the flow temperature.

3.2.1 Operation maps: unit 1

In this research, the performance characteristics of the GEHP system for cooling and heating application are analysed.

Experiments in cooling mode were carried out with an engine load from 100% to 25%, set-point at 7°C, and ambient air temperature from 0°C to 45°C. Furthermore, experiments in heating mode were carried out with an engine load from 100% to 25%, set-point at 45°C, and ambient air temperature from -10°C to 20°C.

These experimental results coincide with the trends of other published studies such as [24,27,30]. Below, the main results obtained from the experiments carried out are analysed and described: Figure 7 displays how the cooling capacity (left) and the EER (right) vary at different load levels and environmental conditions for a fixed flow temperature of 7°C.

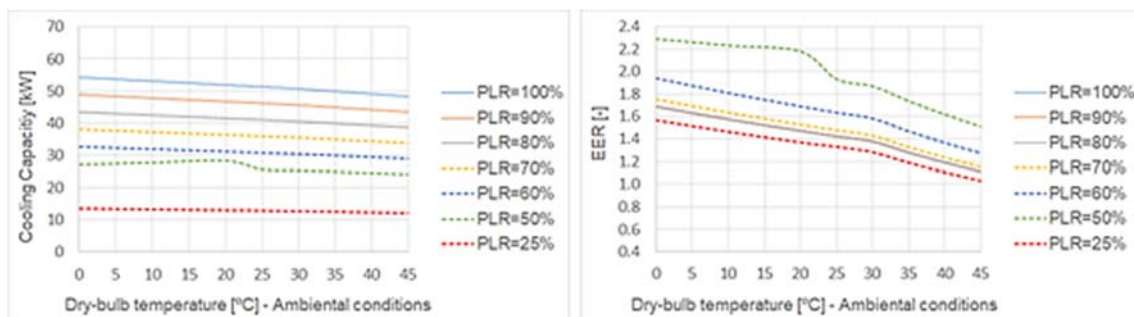


Figure 7. Analysis of Unit ID 1: influence of partial load ratio in cooling mode (set-point 7°C)

Likewise, the heating mode is represented in Figure 8. Heat capacity appears in the left of Figure 8 and the COP performance on the right, at different load regimes and environmental conditions for a flow temperature of 45°C.

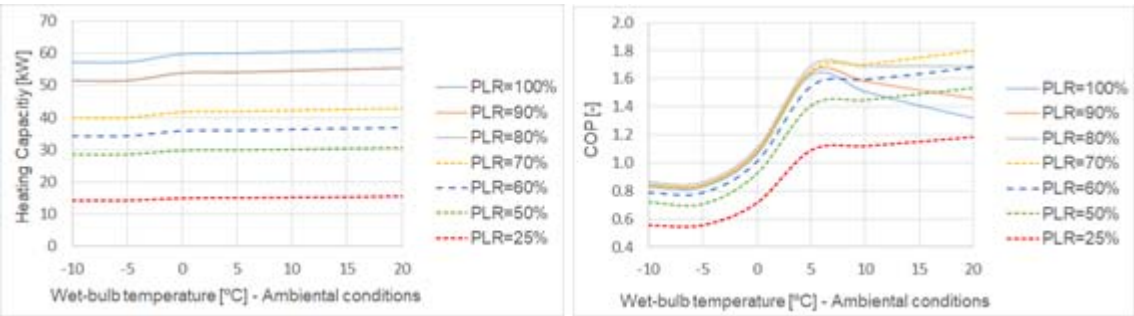


Figure 8. Analysis of Unit ID 1: influence of partial load ratio in heating mode (set-point 45°C)

The other useful heat flux of the system is heat recovered in the engine (jackets and exhaust gases). Variation of this heat flux with the machine load regime and environmental conditions are displayed in Figure 9.

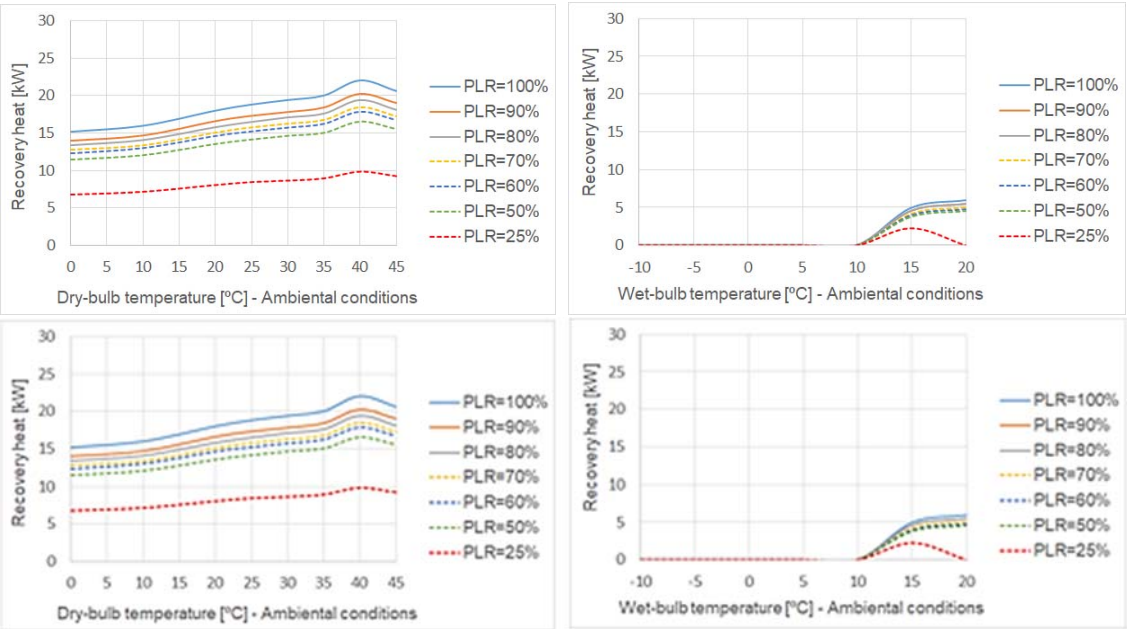


Figure 9. Analysis of Unit ID 1: recovery heat in cooling mode (left, set-point 7°C) and heating mode (right, set-point 45°C)

On the left of Figure 9 is the cold mode, with a flow temperature of 7°C. On the right is the heating mode with a flow temperature of 45°C. It should be noted that when environmental conditions are cold, engine heat is no longer recovered. That is why in heating mode in Figure 9 (right), the power recovered is much lower than that recoverable in cooling mode (left). Additionally, the drop in heat recovered for temperatures above 40°C (left, cooling mode, figure 9) is due to the engine safety systems activating the dissipation mode. This mode operates discreetly at various speeds and at these temperatures, the sensor activates the maximum speed in order to reduce the amount recovered by the water flow in the engine jackets.

Finally, figure 10 displays the electrical consumption of the system in cold (left) and heat (right) modes.

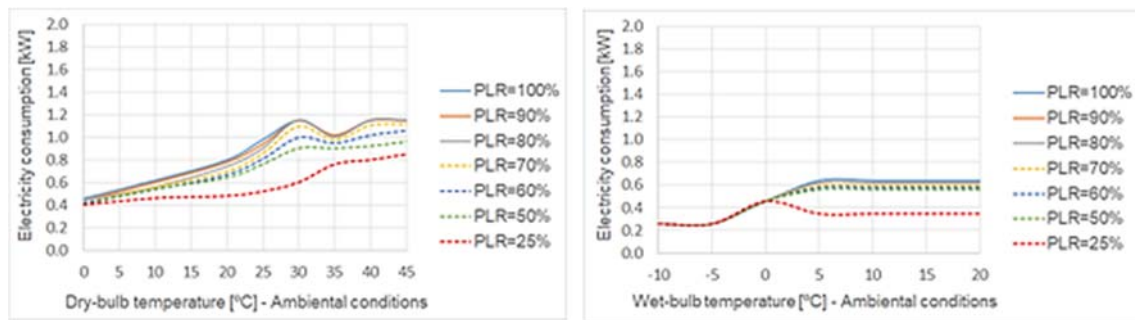


Figure 10. Analysis of Unit ID 1: electricity consumption in cooling mode (left, set-point 7°C) and heating mode (right, set-point 45°C)

The electrical consumption (Figure 10) of these units is low, as it only references the motor dissipation fans and internal electronics of the system.

Effect of ambient air temperature in cooling mode

When the ambient air temperature increases, the variation of energy is illustrated in Figure 7. Also, cooling capacity decrease (Figure 7 - left) while energy consumption increases (Figure 10 - left) when the ambient air temperature increases. Cooling capacity decrease but the specific compressor power increases. Therefore, EER decreases by as shown in Figure 7 (right). The recovery heat to full charge increased from 32 kW to 44 kW as the ambient air temperature increased from 0 °C to 45 °C (Figure 9 - left).

Effect of gas engine speed in cooling mode

When the gas engine speeds increases, the working fluid mass flow, rate load of compressor and compressor speeds are also increased, therefore the cooling capacity, energy consumption and compressor power increase with the increase of gas engine speeds.

The gas engine recovery heat increased from 9.3 kW to 20.6 kW as the gas engine speed increased 25 % to 100 % of charge (figure 9 - left). The reason is that the cooling capacity and shaft power of the compressor increase with the gas engine speeds increasing.

Effect of ambient air temperature in heating mode

When the ambient air temperature increases from -10°C to 20°C, the total heating capacity (Figure 8 - left) and electricity consumption (Figure 10 - right) increase by 7% and 6% respectively.

As evaporating temperature rises, the compression ratios decrease. Also, the refrigerant mass flow increases with the evaporate temperature increases. Therefore, analysis shows that both condenser heat and energy consumption increase, as the ambient air temperature increases.

Since the variation trend of energy consumption is less than the trends of total heating capacity and condenser heat, the performance of GEHP system would improve. Just as it is shown in Figure 8 (right), the COP and of the system go up by 0.8 and 1.3 with the ambient air temperature changing from -10°C to 20°C.

Effect of gas engine speed in heating mode

The total heating capacity (Figure 8 - left), the waste heat (Figure 9 - right) and the energy consumption of the GEHP system (Figure 10 - right) increased as the gas engine speeds

increased. Figure 9 (right) indicates that the waste heat increases slowly with the rise of speed when part load ratio is higher than 25%.

The COP indicates two different trends (Figure 8 - right): for PLR greater than or equal to 80%, the warmer the environment, the lower the COP. On the other hand, this drop is compensated as the load factor of the machine is reduced, therefore, at 70% the COP remains constant at high temperatures.

3.2.2 Units comparison

For these comparisons, all the machines from the same manufacturer have been selected, i.e., units ID 3, 4 and 5 according to table 1 and **¡Error! No se encuentra el origen de la referencia.**table 2. For these comparisons, EER and COP efficiency parameters referencing the cooling cycle, normalised with respect to the nominal value provided in the manufacturer's catalogue, have been selected.

Figure 11 displays the comparison in cooling mode for a flow temperature of 7°C, an external environment dry temperature of 30°C and different load levels from 30% to 100%.

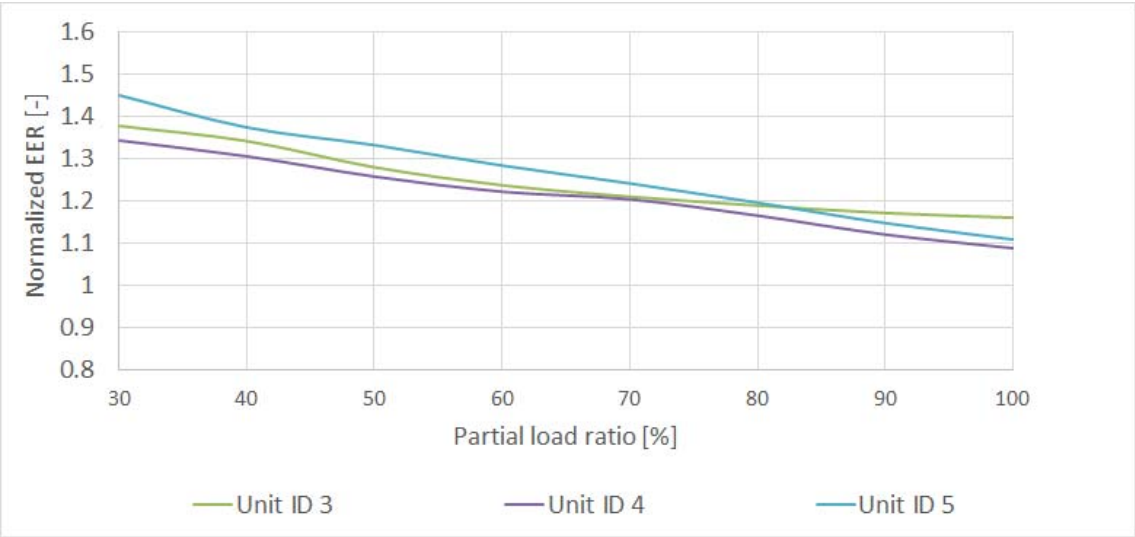


Figure 11. Variation of EER in different partial load ratios (set-point=7°C, Dry-bulb temperature=30°C)

Figure 11 demonstrates that at a low load level, the performance of the machines is better than the nominal value. Along this line, the machines behave the same. However, the larger unit (unit id 5) offers significantly better performance.

Likewise, the heating mode analysis is displayed in Figure 12. In this case, a flow temperature of 35°C with ambient humid temperature conditions of 5°C is used.

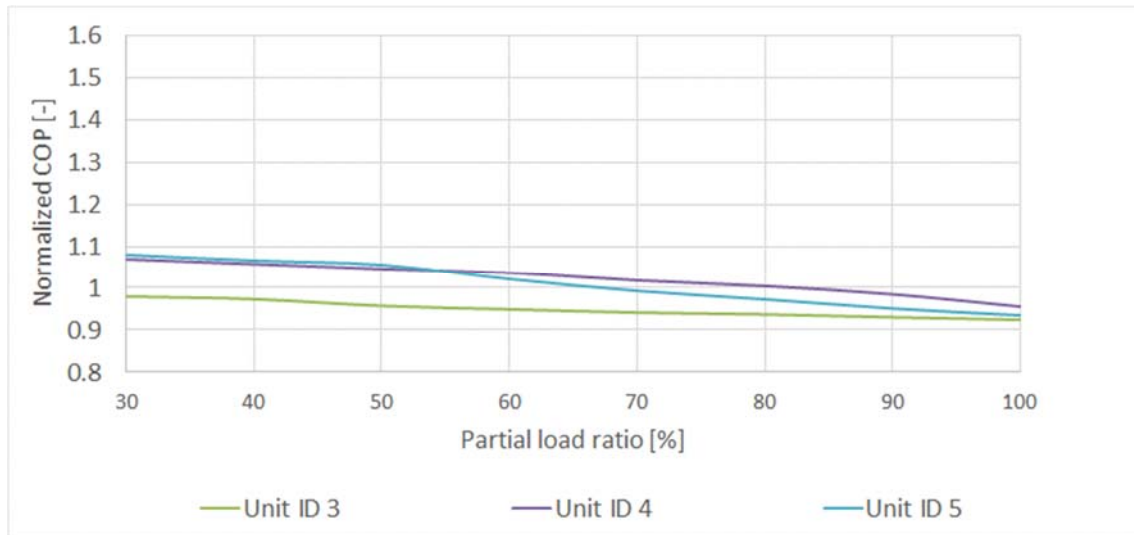


Figure 12. Variation of COP in different partial load ratios (set-point=45°C, Dry-bulb temperature=10°C)

It is important to highlight, as indicated in the previous figures, there is a wealth of experimental data that enables a wide range of behaviour curves. These curves enable thermal characterisation of this type of system.

3.3 Identification of performance curves

Validation has been done by the comparison between experimental data and the estimation of proposed curves.

First, table 11 shows the range in which the curves have been obtained.

Table 11. Range of variable

Parameter		Minimum value	Maximum Value
Engine conditions	PLR partial Load Ratio [%]	25	100
Outside conditions	Dry-bulb temperature [°C] - Cooling Mode	10	45
	Wet-bulb temperature [°C] - Heating Mode	-10	20
Heat production	Outlet water temperature [°C] - Cooling Mode	4	20
	Outlet water temperature [°C] - Heating Mode	35	55
	Outlet water temperature [°C] - Recovery system	-	65

The heating power range has a minimum value of 47 kW and a maximum of 80 kW. For cooling, the minimum value is 41 kW, and the maximum is 71 kW. Additionally, if the machine operates in DHW mode, producible heat is obtained in the condenser, as well as recoverable power in the engine.

Table 12 displays the analysis of obtained adjustments with the characterisation curves. Regression coefficient (R^2) is used for evaluating quality of identified curves. The regression coefficient represents the relationship between estimated and measured data in linear mode. It must have values between 0.7 and 1 to indicate good results [50].

Table 12. Coefficient of determination for performance curves

Name of curve	Unit 1	Unit 2	Unit 3	Unit 4	Unit 5	Generic
COOLCAPT	0.99	0.99	0.99	0.99	0.99	0.93
HEATCAPT	0.99	0.99	0.99	0.99	0.99	0.92

COLDCONT	0.87	0.88	0.91	0.87	0.92	0.83
COLDCONPLR	0.87	0.86	0.81	0.89	0.88	0.86
HEATCONT	0.89	0.90	0.93	0.89	0.94	0.82
HEATCONPLR	0.90	0.88	0.94	0.93	0.89	0.91
REC COLDCAPT	0.91	0.93	0.9	0.92	0.93	0.87
RECCOLDCAPPLR	0.86	0.82	0.87	0.80	0.82	0.81
RECHEATCAPT	0.93	0.95	0.92	0.94	0.95	0.88
RECHEATCAPPLR	0.88	0.82	0.88	0.82	0.83	0.83
COLDECONT	0.82	0.84	0.81	0.83	0.84	0.81
COLDCONPLR	0.84	0.87	0.85	0.86	0.88	0.86
HEATECONT	0.91	0.93	0.90	0.92	0.93	0.88
HEATECONPLR	0.86	0.89	0.86	0.86	0.90	0.83

As displayed in Table 12, the curve adjustments made are acceptable. Additionally, Table 12 displays the generic unit proposal in the last column. This generic unit is the result of the adjustment of behaviour curves using the experimental data of the five units studied. The objective is to demonstrate that the proposed formulation may be used in specific units or with a sample of experimental data from a set of machines. This application may be used for regulatory or decision-making procedures.

In order to complete this information, appendix shows values of curves coefficients for studied units and proposed generic unit. Additionally, section 3.4 shows the results of the execution of these curves in conditions other than those used for identification

3.4 Validation

To do the validation, the experimental sample presented in section 3.2 “Experimental Results” has been expanded. This extension has consisted of testing the same machines with the same load levels and same external conditions (see table 9 and 10), but with different water production temperatures. In cooling mode, it adds cases with 10 and 14 °C of water outlet temperature (7 and 18 °C have been used to identify operation curves). Also, 38, 42 and 48 °C have been added in heating mode (35 and 45 °C have been used to identify operation curves).

Thus, coefficients of curves have been identified using experimental data of tables 9 and 10; and the validation has been done with this new data. For the analysis, COP and EER have been chosen as variables. These variables take into account: characterization of thermal power delivered by the primary in different working conditions (numerator); and gas consumption in these variable working conditions (denominator).

Figure 13 shows the comparison between these new measured COP and EER data, and estimation made with the curves associated with each of the machines. The maximum error is 20% for the cases of EER and 27% for COP cases. The average error is less than 7% in both cases.

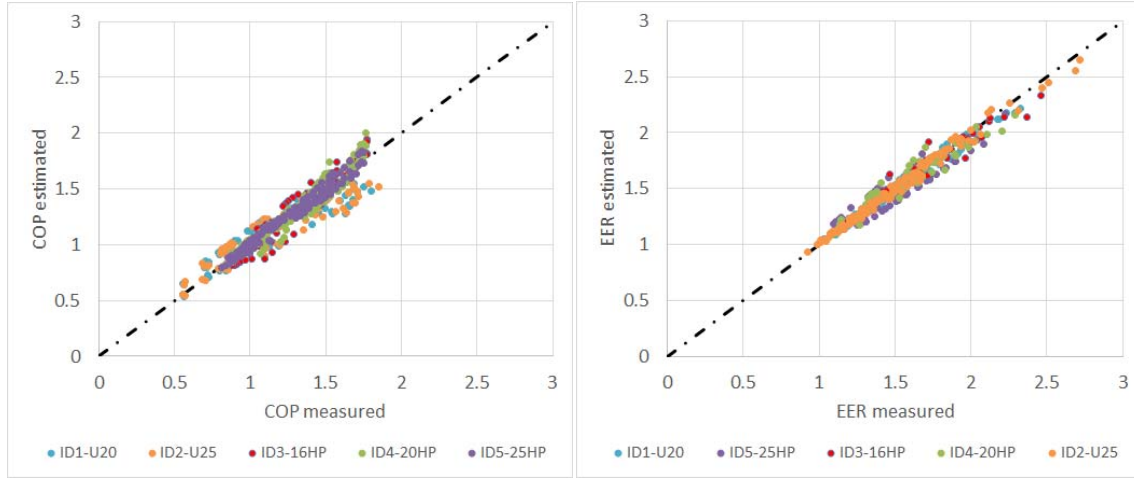


Figure 13. Comparison COP (left) and EER (right) measured and estimated using the different unit curves

Besides, it has been defined as generic curves in this work. The coefficients of these generic curves, as commented, have been obtained using all the experimental data of section 3.2. These curves seek to increase the replicability of the process and can serve as representative curves. Figure 14 shows the results of the estimations made with the generic curves on the 5 machines. There are 5 points with errors higher than 30%, but in general, errors are controlled and less than 15%. It should be noted that they are somewhat superior to those estimated using the curves of each of the units.

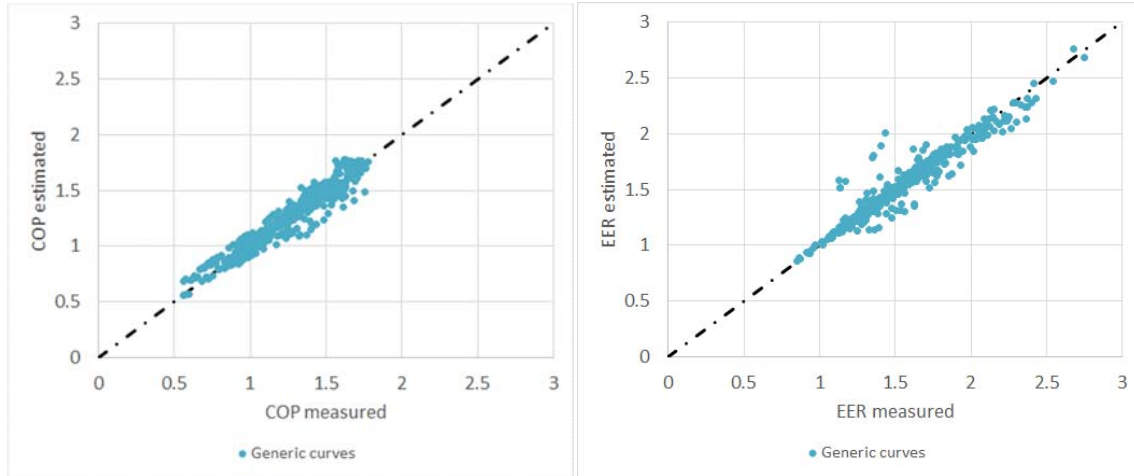


Figure 14. Comparison COP (left) and EER (right) measured and estimated using generic curves for all the data (5 tested units)

Results (see figure 13 and 14) give confidence about the performance curves. Therefore, the proposal made in this paper could be used by the research community to analyse the actual gas engine heat pump.

Also, it has been done a Taylor series method for uncertainty propagation [51]. This method proposes calculating error in the estimation by eq. 19.

$$F_{ESTIMATED} = F_{CURVES} \mp \Delta F \quad \text{Eq. (19)}$$

Where $F_{ESTIMATED}$ is the final estimation for the curve factors, F_{CURVES} is the result of curves (section 2.4 Experimental performance curves), and ΔF is the calculated uncertainty for each curves using eq. 20.

$$\Delta F = \left| \frac{\partial f}{\partial X_1} \right| \cdot \sigma(X_1) + \left| \frac{\partial f}{\partial X_2} \right| \cdot \sigma(X_2) \quad \text{Eq. (20)}$$

Where $\sigma(X_1)$ and $\sigma(X_2)$ are typical uncertainty of the independent variables in performance curves (section 2.4). These values are linked to the accuracy of the sensors (see section 3.1).

Finally, table 13 compares values of average uncertainty, that they have been calculated using eq. 20 (expected value) and, the average relative error of measurements (real value, $F_{\text{TRUE}}/F_{\text{ESTIMATED}}$).

Table 13. Results of validation: provided and average measured uncertainty associated with each proposed curve

$\Delta F[\%]$	Unit 1		Unit 2		Unit 3		Unit 4		Unit 5		Generic	
COOLCAPT	6.2	7.9	8.4	9.7	6.7	8.3	7.1	9.5	6.9	9.2	8.0	10.7
HEATCAPT	5.6	7.1	8.2	9.2	6.6	7.8	6.7	9.1	6.3	8.6	7.1	9.4
COLDCONT	6.8	8.8	8.6	10.2	6.8	8.8	7.5	9.9	7.6	9.8	9.0	12.2
COLDCONPLR	6.9	8.8	9.3	10.8	7.4	9.2	7.9	10.6	7.7	10.2	8.9	12.0
HEATCONT	6.4	8.1	8.6	9.9	6.8	8.5	7.3	9.7	7.1	9.4	8.2	10.9
HEATCONPLR	6.3	7.9	9.2	10.3	7.3	8.7	7.5	10.2	7.0	9.6	8.0	10.5
REC COLDCAPT	7.8	10.1	9.7	11.6	7.7	10.0	8.5	11.2	8.6	11.2	10.2	13.9
RECCOLDCAPLR	8.0	10.4	10.0	11.9	8.0	10.3	8.8	11.6	8.9	11.5	10.5	14.4
RECHEATCAPT	7.1	9.0	9.5	11.0	7.6	9.4	8.1	10.8	7.9	10.5	9.1	12.2
RECHEATCAPLR	7.2	9.2	9.7	11.2	7.8	9.6	8.2	11.0	8.0	10.7	9.3	12.5
COLDECONT	8.8	11.7	10.2	12.5	8.1	10.9	9.3	12.0	9.8	12.3	11.8	16.4
COLDCONPLR	7.9	10.3	9.9	11.8	7.9	10.2	8.7	11.4	8.8	11.4	10.4	14.2
HEATECONT	7.7	9.9	9.6	11.4	7.6	9.8	8.4	11.0	8.5	11.0	10.1	13.7
HEATECONPLR	7.8	10.2	9.8	11.6	7.8	10.1	8.6	11.3	8.7	11.3	10.3	14.0

Uncertainty analysis is a good indicator of confidence in the model [52]. Best way to evaluate uncertainty depends on the models and available information [53], for that, Taylor's method has been chosen for its simplicity and clarity. Results of table 13 can guarantee that uncertainty is controlled in average value. Maximum error is upper of 30% in certain points, for example, in the electrical consumption curves. However, a combination of curves allows evaluating energy flows of the units tested with low errors, and proposed generic curves can be used with any other unit.

4 Conclusions

This paper develops an experimental analysis of gas engine heat pump. Thanks to these experimental data, it has been possible to know the real operation of GEHP and comparison different units. Besides, it proposes a simplified model using experimental results. This model is based on operating curves validated by experimental data from five different units tested under different operating conditions. The model proposed is highly accurate, easy to reproduce, and can be adapted for any system of gas engine heat pump (generic curves). This model could be integrated into a higher-order air conditioning scheme.

The results demonstrate that:

- The set of proposed operating curves enables characterisation of energy flows, electricity and fuel consumption of systems based on gas heat pump as a function of climatic and operating conditions. The corresponding formulation and values are obtained from their

coefficients by adjustments using experimental data demonstrate that the results of the estimates are acceptable.

- This ensures proper estimates due to the full range of validity of the proposed model with precise results. Five selected machines from two manufacturers of these technologies have been analysed and cross-testing of these models has also been carried out.
- Results allow guaranteeing robustness and confidence in the model. Since the uncertainty analysis carried out, both theoretically and experimentally, shows how errors are controlled and bounded.

The ability to take advantage of this heat from the thermal engine marks one of the main differences with electric heat pumps since. Also, GEHP allows to obtain free DHW in winter, and the unit is maintained at full performance even with low outdoor temperatures.

Finally, the proposed procedure for the characterisation of heat and cold generation technologies based on gas heat pumps, in addition to providing a solution for the modelling of these technologies, may be used as a methodology for the evaluation and diagnosis of these units. In the case that these technologies are in real operation, the values obtained by monitoring them may be compared with the estimates carried out with the proposed curves under the same conditions.

5 Acknowledgements

The authors would like to take this opportunity to thank SEDIGAS (the Spanish Gas Association) and manufactured companies (PANASONIC and AISIN) for our fruitful long-term cooperation to promote the deregulation of the market and its role as a critical element in the economic development and quality of life of future generations. Finally, the DACAR project “Zero-Energy Balance Districts Through Algorithms of Adaptive Comfort and Optimal Management of Energy Networks” (BIA2016-77431-C2-2-R) funded by Ministry of Economy and Competitiveness (Government of Spain) and European Regional Development's funds (ERDF) for its partial support.

6 Bibliography

- [1] EU. Directive (EU) 2018/2001 of the European Parliament and of the Council on the promotion of the use of energy from renewable sources. Off J Eur Union 2018;2018:82–209.
- [2] Elgendy E, Schmidt J, Khalil A, Fatouh M, Gungor A, Erbay Z, et al. Research on improving energy efficiency and the annual distributing structure in electricity and gas consumption by extending use of GEHP. *Energy* 2013;35:522–31. doi:10.1016/j.ijrefrig.2015.08.023.
- [3] Hepbasli A, Erbay Z, Icier F, Colak N, Hancioglu E. A review of gas engine driven heat pumps (GEHPs) for residential and industrial applications. *Renew Sustain Energy Rev* 2009;13:85–99. doi:10.1016/j.rser.2007.06.014.
- [4] Pezzola L, Danti P, Magnani S. Performance Comparison among Gas Heat Pump, Electric Heat Pump and Conventional Thermal Devices in Tertiary Sector Applications. *Energy Procedia* 2016;101:416–23. doi:10.1016/j.egypro.2016.11.053.
- [5] Kamal R, Narasimhan AK, Wickramaratne C, Bhardwaj A, Goswami DY, Stefanakos EK, et al. Field performance of gas-engine driven heat pumps in a commercial building. *Int J Refrig* 2016;68:15–27. doi:10.1016/j.ijrefrig.2016.04.019.
- [6] Liu H, Zhou Q, Zhao H, Wang P. Experiments and thermal modeling on hybrid energy

802 supply system of gas engine heat pumps and organic Rankine cycle. *Energy Build*
803 2015;87:226–32. doi:10.1016/j.enbuild.2014.11.046.

804 [7] Wan X, Cai L, Yan J, Ma X, Chen T, Zhang X. Power management strategy for a parallel
805 hybrid-power gas engine heat pump system. *Appl Therm Eng* 2017;110:234–43.
806 doi:10.1016/j.applthermaleng.2016.07.138.

807 [8] Chen T, Cai L, Wan X, Ma X, Yan J, Zhang X. Modeling and dynamic energy management
808 control of hybrid-power gas engine heat pump system. *Appl Therm Eng* 2017;121:585–
809 94. doi:10.1016/j.applthermaleng.2017.04.107.

810 [9] Ma X, Cai L, Meng Q, Chen T, Zhang X. Dynamic optimal control and economic analysis of
811 a coaxial parallel-type hybrid power gas engine-driven heat pump. *Appl Therm Eng*
812 2018;131:607–20. doi:10.1016/j.applthermaleng.2017.12.011.

813 [10] Zhang Q, Yang Z, Gao Y De. The multi-goal optimal analysis of stand-alone gas engine
814 heat pump system with energy storage (ESGEHP) system. *Energy Build* 2017;139:525–34.
815 doi:10.1016/j.enbuild.2017.01.039.

816 [11] Zhang Q, Yang Z, Li N, Feng R, Gao Y. The influence of building using function on the
817 operating characteristics of the gas engine driven heat pump with energy storage system
818 (ESGEHPs). *Energy Build* 2018. doi:10.1016/j.enbuild.2018.02.039.

819 [12] Liu F, Dong F, Li Y, Jia L. Study on the heating performance and optimal intermediate
820 temperature of a series gas engine compression-absorption heat pump system. *Appl*
821 *Therm Eng* 2018;135:34–40. doi:10.1016/j.applthermaleng.2018.02.010.

822 [13] Hao H, Yao J, Feng G, Wen H. The Analysis of the Performance of Heating and the
823 Economical Efficiency of the Solar Energy and Gas Heat Pump. *Procedia Eng*
824 2015;121:1490–6. doi:10.1016/j.proeng.2015.09.075.

825 [14] Hao H, Mao L, Feng G, Wen H. Study on Simulation Performance of Solar Energy and Gas
826 Heat Pump for Heating Supply. *Procedia Eng* 2015;121:1482–9.
827 doi:10.1016/j.proeng.2015.09.074.

828 [15] Zhang Q, Yang Z, Li N, Feng R, Shi P. A novel solar photovoltaic/thermal assisted gas
829 engine driven energy storage heat pump system (SESGEHPs) and its performance
830 analysis. *Energy Convers Manag* 2019;184:301–14.
831 doi:10.1016/j.enconman.2019.01.039.

832 [16] Meng Q, Cai L, Ji W, Yan J, Zhang T, Zhang X. Modeling and Optimization of a Hybrid-
833 power Gas Engine-driven Heat Pump. *Procedia Eng* 2016;146:400–9.
834 doi:10.1016/j.proeng.2016.06.421.

835 [17] Li YL, Zhang XS, Cai L. A novel parallel-type hybrid-power gas engine-driven heat pump
836 system. *Int J Refrig* 2007;30:1134–42. doi:10.1016/j.ijrefrig.2007.03.004.

837 [18] Gungor A, Tsatsaronis G, Gunerhan H, Hepbasli A. Advanced exergoeconomic analysis of
838 a gas engine heat pump (GEHP) for food drying processes. *Energy Convers Manag*
839 2015;91:132–9. doi:10.1016/j.enconman.2014.11.044.

840 [19] Sanaye S, Chahartaghi M, Asgari H. Dynamic modeling of Gas Engine driven Heat Pump
841 system in cooling mode. *Energy* 2013;55:195–208. doi:10.1016/j.energy.2013.03.074.

842 [20] Zhao Y, Haibo Z, Zheng F. Modeling and dynamic control simulation of unitary gas engine
843 heat pump. *Energy Convers Manag* 2007;48:3146–53.
844 doi:10.1016/j.enconman.2007.01.033.

845 [21] Sanaye S, Meybodi MA, Chahartaghi M. Modeling and economic analysis of gas engine
846 heat pumps for residential and commercial buildings in various climate regions of Iran.
847 Energy Build 2010;42:1129–38. doi:10.1016/j.enbuild.2010.02.004.

848 [22] Trnsys n.d. <http://www.trnsys.com/>.

849 [23] DOE. EnergyPlus - Engineering Reference 2010.

850 [24] Naldi C, Dongellini M, Morini GL. Climate influence on seasonal performances of air-to-
851 water heat pumps for heating. Energy Procedia 2015;81:100–7.
852 doi:10.1016/j.egypro.2015.12.064.

853 [25] Dongellini M, Naldi C, Morini GL. Seasonal performance evaluation of electric air-to-
854 water heat pump systems. Appl Therm Eng 2015;90:1072–81.
855 doi:10.1016/j.applthermaleng.2015.03.026.

856 [26] Shang S, Li X, Wu W, Wang B, Shi W. Energy-saving analysis of a hybrid power-driven heat
857 pump system. Appl Therm Eng 2017;123:1050–9.
858 doi:10.1016/j.applthermaleng.2017.04.151.

859 [27] Kamal R, Narasimhan AK, Wickramaratne C, Bhardwaj A, Goswami DY, Stefanakos EK, et
860 al. Field performance of gas-engine driven heat pumps in a commercial building. Int J
861 Refrig 2016;68:15–27. doi:10.1016/j.ijrefrig.2016.04.019.

862 [28] Department of Energy - United States of America n.d.
863 <http://apps1.eere.energy.gov/buildings/energyplus/>.

864 [29] Hu B, Li C, Yin X, Cao F, Shu P. Thermal modeling and experimental research of a gas
865 engine-driven heat pump in variable condition. Appl Therm Eng 2017;123:1504–13.
866 doi:10.1016/j.applthermaleng.2017.05.189.

867 [30] Liu H, Zhou Q, Zhao H. Experimental study on cooling performance and energy saving of
868 gas engine-driven heat pump system with evaporative condenser. Energy Convers
869 Manag 2016;123:200–8. doi:10.1016/j.enconman.2016.06.044.

870 [31] Liu FG, Tian ZY, Dong FJ, Cao GZ, Zhang R, Yan A Bin. Experimental investigation of a gas
871 engine-driven heat pump system for cooling and heating operation. Int J Refrig
872 2018;86:196–202. doi:10.1016/j.ijrefrig.2017.10.034.

873 [32] Liu FG, Tian ZY, Dong FJ, Cao GZ, Zhang R, Yan A Bin. Experimental investigation of a gas
874 engine-driven heat pump system for cooling and heating operation. Int J Refrig
875 2018;86:196–202. doi:10.1016/j.ijrefrig.2017.10.034.

876 [33] Elgendy E, Schmidt J. Optimum utilization of recovered heat of a gas engine heat pump
877 used for water heating at low air temperature. Energy Build 2014;80:375–83.
878 doi:10.1016/j.enbuild.2014.05.054.

879 [34] Zhang X, Yang Z, Wu X, Su X-C. Evaluation method of gas engine-driven heat pump water
880 heater under the working condition of summer. Energy Build 2014;77:440–4.
881 doi:10.1016/j.enbuild.2014.03.067.

882 [35] Liu FG, Tian ZY, Dong FJ, Yan C, Zhang R, Yan A Bin. Experimental study on the
883 performance of a gas engine heat pump for heating and domestic hot water. Energy Build
884 2017;152:273–8. doi:10.1016/j.enbuild.2017.07.051.

885 [36] Shah NN, Huang MJ, Hewitt NJ. Performance analysis of diesel engine heat pump
886 incorporated with heat recovery. Appl Therm Eng 2016;108:181–91.
887 doi:10.1016/j.applthermaleng.2016.07.123.

888 [37] Wu J, Ma Y. Experimental study on performance of a biogas engine driven air source heat
889 pump system powered by renewable landfill gas. *Int J Refrig* 2016;62:19–29.
890 doi:10.1016/j.ijrefrig.2015.08.023.

891 [38] Wang M, Chen Y, Liu Q. Experimental study on the gas engine speed control and heating
892 performance of a gas Engine-driven heat pump. *Energy Build* 2018;178:84–93.
893 doi:10.1016/j.enbuild.2018.08.041.

894 [39] Wang M, Yang Z, Su X, Zhang B, Wu X, Shi Y. Simulation and experimental research of
895 engine rotary speed for gas engine heat pump based on expert control. *Energy Build*
896 2013;64:95–102. doi:10.1016/j.enbuild.2013.04.003.

897 [40] Commission THEE. L 239/136 2013:136–61.

898 [41] Pérez-Lombard L, Ortiz J, Maestre IR, Coronel JF. Constructing HVAC energy efficiency
899 indicators. *Energy Build* 2012;47:619–29. doi:10.1016/j.enbuild.2011.12.039.

900 [42] Alves O, Monteiro E, Brito P, Romano P. Measurement and classification of energy
901 efficiency in HVAC systems. *Energy Build* 2016;130:408–19.
902 doi:10.1016/j.enbuild.2016.08.070.

903 [43] Zhang Q, Yang Z, Li N, Feng R, Gao Y. The influence of building using function on the
904 operating characteristics of the gas engine driven heat pump with energy storage system
905 (ESGEHPs). *Energy Build* 2018;167:136–51. doi:10.1016/j.enbuild.2018.02.039.

906 [44] DOE2.com Home Page n.d. <http://www.doe2.com/> (accessed December 28, 2018).

907 [45] Riederer P. Thermal Room Modeling Adapted To The Test Of HVAC Control Systems
908 2001;37:777–90.

909 [46] Peris B, Navarro-Esbrí J, Molés F, Martí JP, Mota-Babiloni A. Experimental
910 characterization of an Organic Rankine Cycle (ORC) for micro-scale CHP applications. *Appl*
911 *Therm Eng* 2015;79:1–8. doi:10.1016/j.applthermaleng.2015.01.020.

912 [47] Velasco Gómez E, Tejero González A, Rey Martínez FJ. Experimental characterisation of
913 an indirect evaporative cooling prototype in two operating modes. *Appl Energy*
914 2012;97:340–6. doi:10.1016/j.apenergy.2011.12.065.

915 [48] Kottek M, Grieser J, Beck C, Rudolf B, Rubel F. World map of the Köppen-Geiger climate
916 classification updated. *Meteorol Zeitschrift* 2006;15:259–63. doi:10.1127/0941-
917 2948/2006/0130.

918 [49] Yunus A. Çengel & Michael A. Boles. *Termodinámica* McGraw-Hill. n.d.

919 [50] Söderström T. *System identification*. UK: Prentice Hall International; 1989.

920 [51] Coleman HW, Steele WG. Appendix B: Taylor Series Method (Tsm) for Uncertainty
921 Propagation. *Exp Validation, Uncertain Anal Eng* 2018:311–23.
922 doi:10.1002/9781119417989.app2.

923 [52] Refsgaard JC, van der Sluijs JP, Højberg AL, Vanrolleghem PA. Uncertainty in the
924 environmental modelling process - A framework and guidance. *Environ Model Softw*
925 2007;22:1543–56. doi:10.1016/j.envsoft.2007.02.004.

926 [53] Uusitalo L, Lehtikoinen A, Helle I, Myrberg K. An overview of methods to evaluate
927 uncertainty of deterministic models in decision support. *Environ Model Softw*
928 2015;63:24–31. doi:10.1016/J.ENVSOFT.2014.09.017.

929

APPENDIX: Operation Curves

A. Mathematical formulation

Bi-quadratic

$$Curve_i = P_0 + P_1 \cdot (X1^1 \cdot X2^0) + P_2 \cdot (X1^0 \cdot X2^1) + P_3 \cdot (X1^2 \cdot X2^0) + P_4 \cdot (X1^1 \cdot X2^1) + P_5 \cdot (X1^0 \cdot X2^2)$$

Cubic

$$Curve_i = P_0 + P_1 \cdot (X^1) + P_2 \cdot (X^2) + P_3 \cdot (X^3)$$

Quadratic

$$Curve_i = P_0 + P_1 \cdot (X^1) + P_2 \cdot (X^2)$$

B. Coefficients of experimental performance curves

Name	Form	Description	Independent Variables
COOLCAPT	bi-quadratic	Variation of cooling capacity (PLR=100%) as a function of outlet water temperature and outdoor dry-bulb temperature	f(X1=Tow , X2=Tdr)

Unit	P0	P1	P2	P3	P4	P5
1	0.60980	0.01367	0.01189	-0.00045	0.00035	-0.00023
2	0.64560	0.01674	0.01680	-0.00070	0.00047	-0.00035
3	0.83434	0.00000	0.01841	0.00095	-0.00014	-0.00039
4	0.77431	0.00000	0.02122	0.00095	-0.00015	-0.00043
5	0.79190	0.00578	0.00893	-0.00019	0.00015	-0.00018
Generic	1.05716	0.00000	-0.00178	0.00061	-0.00004	-0.00001

Name	Form	Description	Independent Variables
HEATCAPT	bi-quadratic	Variation of heating capacity (PLR=100%) as a function of outlet water temperature and outdoor wet-bulb temperature	f(Tow , Twb)

Unit	P0	P1	P2	P3	P4	P5
1	0.50540	0.02584	0.00328	-0.00036	0.00000	0.00000
2	0.34350	0.03674	0.00696	-0.00050	0.00000	0.00000
3	1.03489	0.00000	-0.00288	0.00000	0.00000	-0.00002
4	1.02542	0.00000	-0.00143	0.00000	0.00000	-0.00001
5	0.44300	0.03067	0.01718	-0.00040	-0.00026	0.00000
Generic	1.07058	0.00000	0.00357	-0.00004	-0.00001	-0.00006

Name	Form	Description	Independent Variables
COLDCON T	bi-quadratic	Variation of gas consumption in cooling mode (PLR=100%) as a function of outlet water temperature and outdoor dry-bulb temperature	f(Tow , Tdr)

Unit	P0	P1	P2	P3	P4	P5
1	0.81222	0.00000	0.00069	0.00042	0.00000	0.00012
2	0.75870	0.01873	-0.00076	-0.00012	0.00000	0.00022
3	0.25240	0.03885	0.00274	-0.00068	0.00020	0.00000
4	1.21713	0.00000	-0.02508	0.00000	0.00000	0.00054
5	0.71900	0.00469	-0.00997	-0.00033	0.00015	0.00023
Generic	0.81222	0.00000	0.00069	0.00042	0.00000	0.00012

Name	Form	Description	Independent Variables
COLDCONPLR	cubic	Variation of gas consumption in cooling mode as a function of partial load ratio	f(PLR)

Unit	P3	P2	P1	P0
1	-1.59370	3.51510	-1.32740	0.41130
2	-5.22440	10.82100	-5.72920	1.13180
3	-0.79557	1.73773	-0.12780	0.18333
4	-0.54861	1.47396	-0.11711	0.19021
5	-2.56890	5.71440	2.18880	0.46660
Generic	0.70654	-3.30249	7.03230	-3.44537

Name	Form	Description	Independent Variables
HEATCON T	bi- quadratic	Variation of gas consumption in heating mode (PLR=100%) as a function of outlet water temperature and outdoor wet-bulb temperature	f(T _{ow} , T _{wb})

Unit	P0	P1	P2	P3	P4	P5
1	1.85600	-0.02670	-0.08942	0.00034	0.00124	0.00029
2	1.65600	-0.00736	-0.08347	0.00013	0.00118	0.00000
3	1.34289	0.00000	-0.02702	-0.00005	-0.00025	0.00124
4	1.64300	-0.01897	-0.05980	0.00038	0.00017	0.00058
5	1.43900	-0.01052	-0.04892	0.00013	0.00049	0.00032
Generic	1.34289	0.00000	-0.02702	-0.00005	-0.00025	0.00124

Name	Form	Description	Independent Variables
HEATCONPLR	cubic	Variation of gas consumption in heating mode as a function of partial load ratio	f(PLR)

Unit	P3	P2	P1	P0
1	-1.05590	1.60310	0.15110	0.28970
2	-1.06650	1.69790	0.22120	0.16560
3	-0.85200	1.87325	-0.21929	0.22296
4	-0.36694	1.08476	0.13034	0.14888
5	-0.87400	1.37640	0.24390	0.22730
Generic	-0.02904	2.16531	-2.92832	1.79735

Name	Form	Description	Independent Variables
REC COLDCA P T	bi- quadrati c	Variation of heat recovery in cooling mode (PLR=100%) as a function of outlet water temperature and outdoor dry-bulb temperature	f(T _{ow} , T _{dr})

Unit	P0	P1	P2	P3	P4	P5
1	0.99243	0.00000	-0.00867	0.00020	0.00001	0.00026
2	0.99243	0.00000	-0.00867	0.00020	0.00001	0.00026
3	1.26277	0.00000	-0.02602	0.00000	0.00000	0.00056
4	1.26277	0.00000	-0.02602	0.00000	0.00000	0.00056
5	1.26277	0.00000	-0.02602	0.00000	0.00000	0.00056
Generic	0.72208	0.00000	0.00868	0.00039	0.00002	-0.00003

Name	Form	Description	Independent Variables
RECCOLDCAPPLR	cubic	Variation of heat recovery in cooling mode as a function of partial load ratio	f(PLR)

Unit	P3	P2	P1	P0
1	-0.41546	2.78635	-2.70191	1.32965
2	-0.41546	2.78635	-2.70191	1.32965
3	-0.54688	1.47017	-0.11443	0.18961
4	-0.54688	1.47017	-0.11443	0.18961
5	-0.54688	1.47017	-0.11443	0.18961
Generic	-0.28404	4.10252	-5.28938	2.46970

Name	Form	Description	Independent Variables
RECHEATCAPT	bi-quadratic	Variation of recovery heat in heating mode (PLR=100%) as a function of outlet water temperature and outdoor wet-bulb temperature	f(T _{ow} , T _{dr})

Unit	P0	P1	P2	P3	P4	P5
1	0.04191	0.00000	0.03641	0.00002	0.00008	-0.00102
2	0.04191	0.00000	0.03641	0.00002	0.00008	-0.00102
3	-0.10189	0.00000	0.07282	0.00005	0.00016	-0.00233
4	-0.18330	0.00000	0.11172	0.00013	-0.00076	-0.00256
5	-0.18330	0.00000	0.11172	0.00013	-0.00076	-0.00256
Generic	0.18571	0.00000	0.00000	0.00000	0.00000	0.00029

Name	Form	Description	Independent Variables
RECHEATCAPPLR	cubic	Variation of heat recovery in heating mode as a function of partial load ratio	f(PLR)

Unit	P3	P2	P1	P0
1	0.07458	0.09393	2.61711	-16.93921
2	0.11173	0.16955	1.73482	-8.59481
3	0.21281	-0.06572	1.52274	-0.67266
4	0.14887	0.24517	0.85252	-0.25041
5	0.14887	0.24517	0.85252	-0.25041
Generic	0.02334	1.05579	0.02194	-0.11154

Name	Form	Description	Independent Variables
COLDECONT	quadratic	Variation of electricity consumption in cooling mode (PLR = 100%) as a function of outdoor dry-bulb temperature	f(Tdr)

Unit	P2	P1	P0
1	-0.46112	0.06886	-0.00109
2	-1.69531	0.16130	-0.00269
3	0.64459	-0.01644	0.00028
4	0.85369	-0.02124	0.00040
5	-1.63750	0.13656	-0.00219
Generic	0.45367	0.02297	-0.00015

Name	Form	Description	Independent Variables
COLDCONPLR	cubic	Variation of electricity consumption in cooling mode as a function of partial load ratio	f(PLR)

Unit	P3	P2	P1	P0
1	0.07332	0.53436	0.43348	-0.04095
2	-0.40693	2.96228	-3.39177	1.84245
3	-0.19078	1.95915	-1.59652	0.83342
4	0.07332	0.53436	0.43348	-0.04095
5	-0.19078	1.95915	-1.59652	0.83342
Generic	0.52562	0.67958	0.05207	-0.24550

Name	Form	Description	Independent Variables
HEATECONT	quadratic	Variation of electricity consumption in heating mode (PLR = 100%) as a function of outdoor wet-bulb temperature	f(Twb)

Unit	P2	P1	P0
1	0.85369	-0.02124	0.00040
2	0.89771	-0.01500	0.00019
3	0.64459	-0.01644	0.00028
4	0.85369	-0.02124	0.00040
5	0.64459	-0.01644	0.00028
Generic	0.73846	0.03282	-0.00100

Name	Form	Description	Independent Variables
HEATECONPLR	cubic	Variation of electricity consumption in heating mode as a function of partial load ratio	f̂(PLR)

Unit	P3	P2	P1	P0
1	0.15004	0.12615	1.09094	-0.36977
2	0.05629	0.49903	0.62168	-0.17719
3	0.21993	-0.23053	1.85004	-0.84163
4	0.15004	0.12615	1.09094	-0.36977
5	0.21993	-0.23053	1.85004	-0.84163
Generic	0.27827	2.61989	-3.35744	1.47284